temperature. After 3 times of PBS rinses for 5 min, a polyclonal antibody against factor VIII (Invitrogen) was added at a dilution of 1:50, followed by incubation for 1 h and 3 times of PBS rinses for 5 min each. Biotinylated anti-rabbit IgG was added at a dilution of 1:50, followed by incubation for 1 h. The sections were rinsed 3 times with PBS, and Vectastain Elite ABC Reagent (Vector Laboratories, Burlingame, CA, United States of America) was used. The sections were rinsed again 3 times with PBS and incubated with 3,3′-diaminobenzidine tetrahydrochloride (DAB+) Liquid System (Dako) for 30 s. Finally, the sections were rinsed and counterstained with haematoxylin solution.

2.6. *In vivo growth inhibition assay*

2.6.1. *Experiment 1*

Orthotopic mice bearing a pancreatic tumour were randomly divided into four groups consisting of five mice per group. The maximum tolerated doses (MTDs) of NK012 (30 mg/kg at SN-38 equivalents dose, 0.076 mmol/kg) and CPT-11 (66.7 mg/kg; 0.098 mmol/kg) were intravenously injected on days 0 (21 d after tumour inoculation), 4 and 8. The MTD of gemcitabine (16.5 mg/kg) was administrated intraperitoneally on days 0, 3, 6 and 9 as described previously.[20] As a control, normal 0.9% NaCl solution was intravenously administered on days 0, 4 and 8. Kaplan–Meier analysis was performed to determine the effects of the drugs. Statistical differences were ranked according to the Mantel–Cox log-rank test using StatView 5.0. The percentage of Increase in Life Span (ILS%) was calculated as follows[21]: ILS% = $(T/C - 1) \times 100$. T is the median survival days in drug treatment mouse group and C is the median survival days in control mouse group.

2.6.2. *Experiment 2*

To assess the antitumour effects of NK012, CPT-11 and gemcitabine, *in vivo* bioluminescence imaging studies were performed using the Photon Imager animal imaging system (Biospace, Paris, France). For imaging, mice bearing orthotopic pancreatic tumour were simultaneously anesthetised with isoflurane and D-luciferine potassium salt (Synchem, Germany), normal 0.9% NaCl solution was intraperitoneally administrated at 125 mg/kg, and images were taken 5 min postinjection. For bioluminescence image analysis, regions of interest encompassing the area of a signal were defined using Photo Vision software (Biospace), and total numbers of photons per minute (cpm) were recorded. The pseudo-colour luminescent image from violet (least intense) to red (most intense) represented the spatial distribution of detected photon counts emerging from active luciferase within an animal. Twenty-one days after SUIT-2/Luc inoculation, treatment was conducted as described in Experiment 1. *In vivo* bioluminescence imaging studies were performed on days 0, 3, 6, 9 and 12 from the day of treatment initiation. To determine the effects of treatment on the time to change luminescence intensity, ANOVA analysis was carried out using StatView 5.0 software. $P < 0.05$ was considered significant.

2.6.3. *Experiment 3*

Mice bearing orthotopic pancreatic tumour were treated as described in Experiment 1. Twelve days later from treatment initiation, tumours were excised from the pancreas. Thereafter, the length (a) and width (b) of tumour masses were measured; tumour volume was calculated as follows: tumour volume = $(a \times b^2) \times 0.5233$. At the same time, we measured tumour weight.

To evaluate the metastatic nodules of the implanted pancreatic cancer, we measured nodule area in the mesentery.

2.7. *Evaluation of NK012 and CPT-11 distribution in tumour tissue by fluorescence microscopy*

The SUIT-2 orthotopic pancreatic tumour tissues described above were used for the analysis of the biodistributions of NK012 and CPT-11. Twenty-one days after the SUIT-2 cell inoculation, the MTD of NK012 (30 mg/kg) or CPT-11 (66.7 mg/kg) was injected intravenously into the tail vein of mice. 1, 6, 24 and 48 h after NK012 or CPT-11 injection, the mice were administered with fluorescein *Lycopersicon esculentum* lectin (100 μl/mouse) (Vector Laboratories) to visualise tumour blood vessels. After sacrificing the mice under anaesthesia, tumours were then excised and embedded in an optimal cutting temperature compound and were frozen at −80 °C until use. Tissue sections (6 μm thick) were prepared using Tissue-Tek Cryo3 (Sakura Finetek United States of America, Inc., Torrance, CA, United States of America), and the frozen sections were examined under a fluorescence microscope, BIOREVO BZ9000 (Keyence, Osaka, Japan), at an excitation wavelength of 377 nm and an emission wavelength 447 nm to evaluate the distributions of NK012 and CPT-11 within the tumour tissues. Because formulations containing SN-38 bound via ester bonds possess a particular fluorescence, both NK012 and CPT-11 could be detected under the same fluorescence conditions.

2.8. *Pharmacokinetics study of NK012 and CPT-11*

Mice bearing orthotopic SUIT-2 cells were used for the analysis of the biodistributions of NK012 and CPT-11. NK012 (30 mg/kg) and CPT-11 (66.7 mg/kg) were intravenously administered to mice bearing SUIT-2 cells or to normal mice. Mice were sacrificed under anaesthesia, and tumour and normal pancreatic tissues were obtained 1, 6, 24, 48, 72, 96, 120, 144, 168 and 192 h after NK012 or CPT-11 injection. Pharmacokinetics study was conducted as described previously.[14] Briefly, the tumour and normal pancreatic tissues were rinsed with physiological 0.9% NaCl solution, mixed with 0.1 M glycine–HCl buffer (pH 3.0)/methanol at w/w% and then homogenised. To analyse the concentration of free SN-38 and CPT-11, 100 μl of the tumour homogenates was mixed with 20 μl of 1 mM phosphoric acid/methanol (1:1), 40 μl of ultrapure water and 60 μl of camptothecin solution (10 ng/ml for SN-38 and 15 ng/ml for CPT-11) as an internal standard. The samples were vortexed vigorously for 10 s, and then filtered through Ultrafree-MC Centrifugal Filter Devices with a cut-off molecular diameter of 0.45 μm (Millipore Co., Bedford, MA, United States of America). Reversed-phase HPLC was performed at 35 °C on a Mightysil RP-18 GP column (150 × 4.6 mm; Kanto Chemical Co., Inc., Tokyo, Japan). A sample (50 μl) was injected into an Alliance Waters 2795 HPLC system (Waters, Milford, MA, United States of America) equipped

Please cite this article in press as: Saito Y. et al., Antitumour activity of NK012, SN-38-incorporating polymeric micelles, in hypovascular orthotopic pancreatic tumour, *Eur J Cancer* (2009), doi:10.1016/j.ejca.2009.11.014

with a Waters 2475 multi λ fluorescence detector. Fluorescence originating from SN-38 was detected at 540 nm with an excitation wavelength of 365 nm and that originating from CPT-11 was detected at 430 nm with an excitation wavelength of 365 nm. The mobile phase was a mixture of 100 nmol/L ammonium acetate (pH 4.2) and methanol (11:9(v/v)). The flow rate was 1.0 ml/min. SN-38 content was calculated by measuring the relevant peak area and calibrating against the corresponding peak area derived from the CPT-11 internal standard. Peak area was recorded using a chromatography management system (MassLynx v4.0, Waters). In these experiments, limit of the detection of CPT-11 or SN-38 was 0.002 μg/g tumour or0.018 μg /g tumour, respectively.

For polymer-bound SN-38 detection, SN-38 was released from the conjugate. Briefly, 100 μl of tissue samples was diluted with 20 μl of methanol (50 w/w%) and 20 μl of NaOH (0.7 mol/L). The samples were incubated for 15 min at 25 °C. After incubation, 20 μl of HCl (0.7 mol/L) and CPT solution (10 ng/ml for SN-38 and 15 ng/ml for CPT-11) were added to the samples, and then the hydrolysate was filtered through a MultiScreen Solvinert. The filtrate (15 μl) was applied to the same HPLC system described above.

2.9. *Statistical analysis*

Student's t-test was used for the statistical analyses unless otherwise mentioned. $P < 0.05$ was considered significant.

3. Results

3.1. *In vitro cellular sensitivity of SUIT-2 cells to NK012, gemcitabine, CPT-11 and SN-38*

The inhibitory concentration 50% (IC_{50}) values showed that the growth inhibitory effects of NK012 were 100-fold more potent than those of CPT-11 against SUIT-2 cells. On the other hand, the IC_{50} values of NK012 were almost similar to those of SN-38 and gemcitabine (Fig. 1).

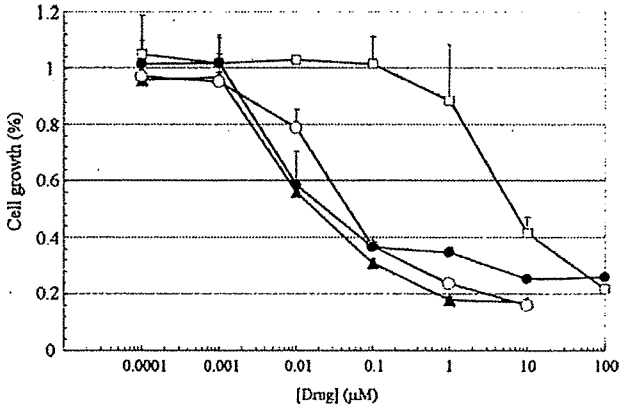

Fig. 1 – *In vitro* growth inhibitory activities of NK012, SN-38, CPT-11 and gemcitabin. Cell growth inhibitory activities of NK012, SN-38, CPT-11 and gemcitabin were measured using the WST-8 assay. SUIT-2 cells (5000 cells/well) in 96-well plates were incubated overnight. Growth medium was changed to new medium with various concentrations of NK012 (○), SN-38 (▲), CPT-11 (□) and gemcitabin (●). Cell viability was measured as described in Section . Points, mean; Bars, SD.

3.2. *Orthotopic SUIT-2 pancreatic tumour and its metastatic nodules in mesentery of mice*

We previously found that NK012 could eradicate human tumour xenografts grown subcutaneously in mice.[19] However, the pathological features of the subcutaneous tumour were different from those of the human pancreatic cancer. Additionally, the latter frequently exhibits extensive invasion into surrounding tissue. To assess the antitumour effects of NK012 in a model similar to human pancreatic cancer, we established orthotopic pancreatic tumour xenografts. We then examined pancreatic tumour growth and spread in the mesentery from 1 to 3 weeks postinjection of SUIT-2 cells into the pancreas (Fig. 2A). The tumour transplanted orthotopically grew from 1 to 3 weeks within the pancreatic body, and thereafter metastatic nodules developed in the mesentery. We also compared the number of blood vessels between an orthotopic tumour and a subcutaneous tumour 3 weeks postinoculation (Fig. 2B). We found that the orthotopic tumour had a smaller number of blood vessels than the subcutaneous tumour.

3.3. *Antitumour activity of NK012, CPT-11 and gemcitabine against SUIT-2 orthotopic pancreatic tumour xenografts*

Kaplan–Meier analysis showed significant improvement in survival rate in the NK012 treatment group (ILS%, 177) than in the control, CPT-11 (ILS% 63) and gemcitabine groups (ILS%, 74) (Fig. 3A). Regarding antitumour activity, a photon imager indicated that NK012 showed the most potent activity amongst all treatment drugs (Fig. 3B). To confirm the antitumour effects obtained by the photon imager, each tumour was excised for tumour volume and weight measurement (Fig. 3C). NK012 also strongly inhibited the metastatic nodule area compared with the control group (Fig. 3D).

3.4. *Studies on distribution and pharmacokinetics analysis of NK012 and CPT-11 in orthotopic pancreatic tumour tissues*

To examine NK012 and CPT-11 distributions, pancreatic tumour tissues were obtained 1, 6, 24 and 48 h after NK012 or CPT-11 injection, and frozen sections were observed under a fluorescence microscope (Fig. 4A). The drug distribution pattern was clearly different between NK012 and CPT-11. In the sections of CPT-11-treated tumour tissues, fluorescence from CPT-11 was observed in the area of entire tumour tissue, and maximum drug accumulation occurred within 1 h of CPT-11 injection. However, 24 h after CPT-11 injection, fluorescence had almost disappeared and no CPT-11 accumulation was observed thereafter. In the sections of NK012-treated tumour tissues, fluorescence from NK012 started appearing within the tumour tissue 1 h after NK012 injection. The fluorescence area started to increase throughout the tumour tissue 6 h postinjection and maximum fluorescence was observed at 24 h. The fluorescence from NK012 continued to be observed

Please cite this article in press as: Saito Y et al., Antitumour activity of NK012, SN-38-incorporating polymeric micelles, in hypovascular orthotopic pancreatic tumour, *Eur J Cancer* (2009), doi:10.1016/j.ejca.2009.11.014

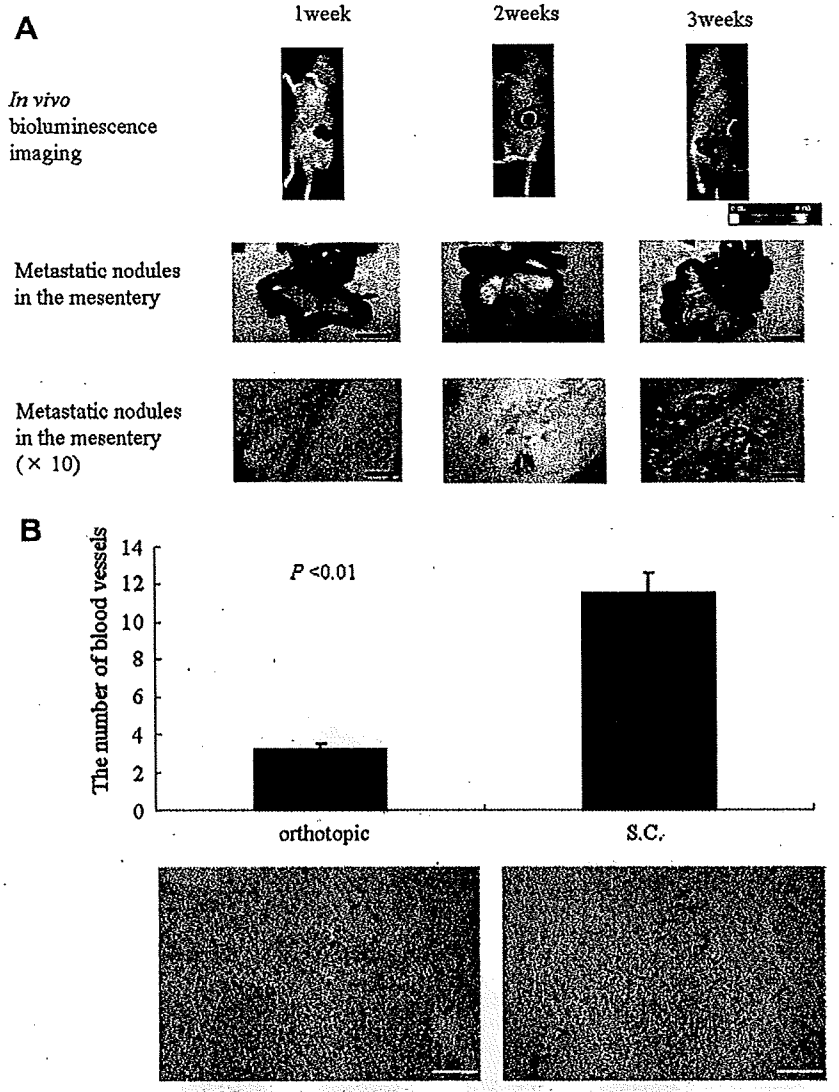

Fig. 2 – Progression of orthotopically implanted SUIT-2 pancreatic tumour xenografts. (A) *In vivo* bioluminescence imaging (upper panels) and metastastic nodules in the mesentery (middle panels: scale bar, 10 mm; lower panels: scale bar, 1 mm). (B) Number of blood vessels in orthotopic tumour xenografts and subcutaneous (S.C.) tumour xenografts. After immunostaining with anti-factor VIII antibody, the number of tumour blood vessels in each xenograft was counted. Column, mean + SD. $P < 0.01$ (orthotopic versus S.C.). Scale bar: 200 μm.

until 48 h. Microscopic observations were confirmed quantitatively by measuring the amount of SN-38 from tumour tissues by reversed-phase HPLC. In the tumour tissues (Fig. 4B), CPT-11 concentration decreased rapidly with time in a log-liner fashion after CPT-11 injection. Free SN-38 (converted from CPT-11) was only detected 1 h after CPT-11 injection. On the other hand, NK012 (polymer-bound SN-38) and free SN-38 (released from NK012) continued to be detected from 1 to 192 h after NK012 injection. Additionally, we compared NK012 concentration between pancreatic tumour tissues and normal pancreatic tissues (Fig. 4C). NK012 concentration in normal pancreatic tissues was significantly lower than that in pancreatic tumour tissues from 1 to 192 h after NK012 injection.

4. Discussion

Here, we used an orthotopic pancreatic tumour model to evaluate the antitumour effects of NK012. The orthotopic pancreatic cancer xenografts showed poorer vasculature and more abundant interstitium than the subcutaneous tumour xenografts. Moreover, peritoneal dissemination accompanied the orthotopic tumour. These results indicate that SUIT-2 orthotopic tumours can be used as a substitute for locally advanced human pancreatic cancer.

NK012 showed more potent antitumour activity and longer survival rate than CPT-11, gemcitabine and control. We observed drug accumulation and distribution within tumour tissues by fluorescence microscopy. Maximum drug accumulation was observed within 1 h of CPT-11 injection. Twenty-four hours after CPT-11 injection, fluorescence from CPT-11 had almost disappeared, whilst that from NK012 started appearing within the tumour tissues 1 h postinjection, and then spread to the entire body of the pancreatic tumour tissues by 48 h postinjection. These microscopic observations were confirmed quantitatively by HPLC. Regarding the distribution of NK012 in normal major organs, it showed relatively

Please cite this article in press as: Saito Y et al., Antitumour activity of NK012, SN-38-incorporating polymeric micelles, in hypovascular orthotopic pancreatic tumour, *Eur J Cancer* (2009), doi:10.1016/j.ejca.2009.11.014

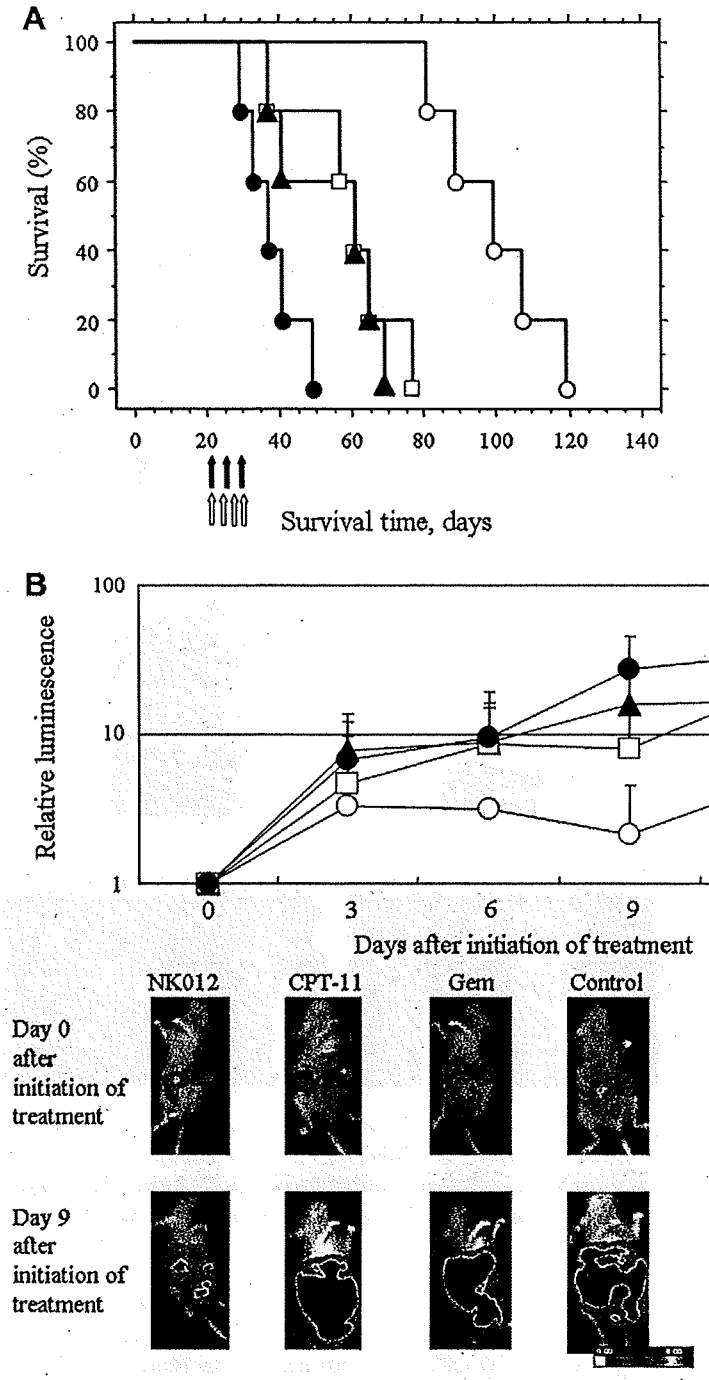

Fig. 3 – Antitumour effects of NK012 in orthotopic tumour xenografts. Mice bearing SUIT-2 tumours were assigned into 4 groups, 21 d after tumour inoculation. Mice were intravenously administered with NK012 (○) (30 mg/kg/d), CPT-11 (▲) (66.7 mg/kg/d) and 0.9% NaCl solution (●) (as a control) on days 0 (21 d after tumour inoculation), 4 and 8. Gemcitabine (□) (16.5 mg/kg/d) was administrated intraperitoneally on days 0, 3, 6 and 9. (A) Effects of NK012 treatment on survival. Survival was assessed by Kaplan–Meier analysis. NK012, CPT-11 and 0.9% NaCl solution were administered on days 0, 4 and 8 (black arrows) and gemcitabine on days 0, 3, 6 and 9 (white arrows). $P < 0.0018$ (NK012 versus CPT-11), $P < 0.0018$ (NK012 versus gemcitabine), $P < 0.0018$ (NK012 versus control). (B) Representative luminescence intensity images obtained in individual control and treatment group mice on days 0 and 9. Points, mean + SD. $P = 0.0074$ (NK012 versus control), $P = 0.0231$ (NK012 versus CPT-11), $P = 0.0239$ (NK012 versus gemcitabine). (C) Tumour volume and tumour weight in mice treated with NK012, CPT-11, gemcitabine and control. Column, mean + SD. $^{*}P < 0.05$ (versus NK012). $^{**}P < 0.01$ (versus NK012). Scale bar, 10 mm. (D) Suppression of metastatic nodules in mesentery by NK012. After 12 d of treatment initiation, the mesentery was dissected and nodule area was measured. Upper panel scale bar, 10 mm; lower panel scale bar, 1 mm. Graph column, mean + SD. $^{**}P < 0.01$ (versus NK012).

Please cite this article in press as: Saito Y. et al., Antitumour activity of NK012, SN-38-incorporating polymeric micelles, in hypovascular orthotopic pancreatic tumour, *Eur. J. Cancer* (2009), doi:10.1016/j.ejca.2009.11.014

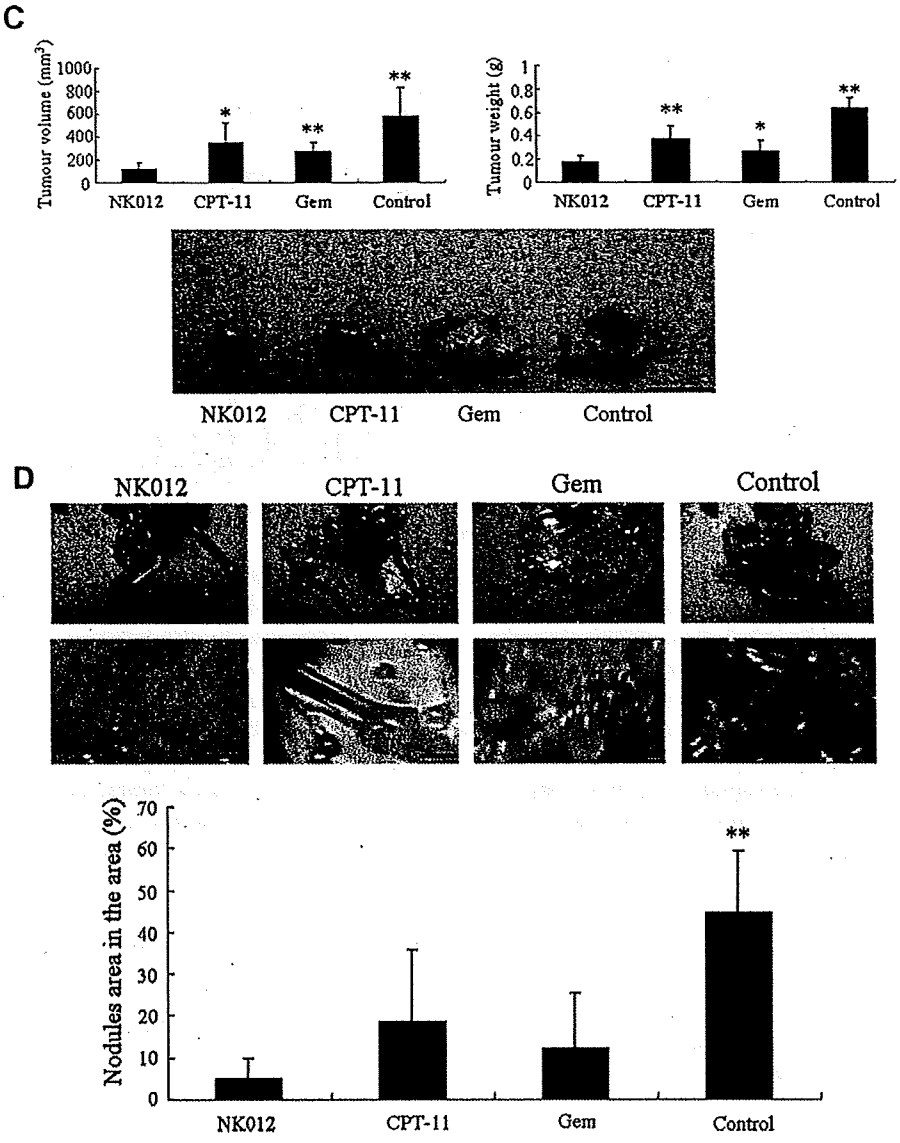

Fig 3. *(continued)*

prolonged distribution in the liver and spleen.[14] However, hepatic toxicity was not observed by a biochemical analysis in the injection of NK012. This long SN-38 retention time is important for its antitumour effects because its antitumour activity is time-dependent.[22] Therefore, we conclude that long-term distribution and retention of NK012 and SN-38 released from NK012 is one of the essential properties underlying the superior antitumour activity of NK012 in such stroma-rich tumours.

In hypervascular tumours, drug formulations categorised in DDS can effectively accumulate in the tumours and sufficiently exert antitumour effect. However, in hypovascular tumours, for example, liposomal drugs can be efficiently delivered to the tumour tissue but free drugs are not sufficiently distributed to cancer cells. Because their formulation is too large to allow penetration of tumour interstitium and is too stable to allow the free drug within liposomes to be released easily. In fact, Doxil[23], a pegylated liposomal doxorubicin, is clinically effective against hypervascular cancers[24,25] such as ovarian tumours, breast cancer and Kaposi sarcoma but not against stomach and pancreatic cancers, both of which have a low density of tumour microvessels. On the other hand, NK012 is small (20 nm)[14] compared with liposomes, which is why it can be distributed more uniformly in the tumour tissue. Furthermore, NK012 has the potential to allow the effective sustained release of free SN-38 inside a tumour following NK012 accumulation in the tumour tissue. Consequently, SN-38 thus released distributes throughout the tumour tissue and is internalised into cancer cells to kill them.

Here, we have shown that NK012 has potent antitumour effects against orthotopic pancreatic tumours compared with gemcitabine and CPT-11, and that NK012 decreased the number of metastatic nodules in the peritoneal cavity. Thus, we admonish that it is better to use orthotopic tumour xenografts to evaluate the antitumour activity against cancer characterised by few tumour vessels and high amount of tumour stroma. Moreover, enhanced accumulation, distribution and retention of polymeric micelle-based anticancer drugs within the tumour tissue and the sustained release of anticancer drugs from the micelles are key elements for the treatment

Please cite this article in press as: Saito Y et al., Antitumour activity of NK012, SN-38-incorporating polymeric micelles, in hypovascular orthotopic pancreatic tumour, *Eur J Cancer* (2009), doi:10.1016/j.ejca.2009.11.014

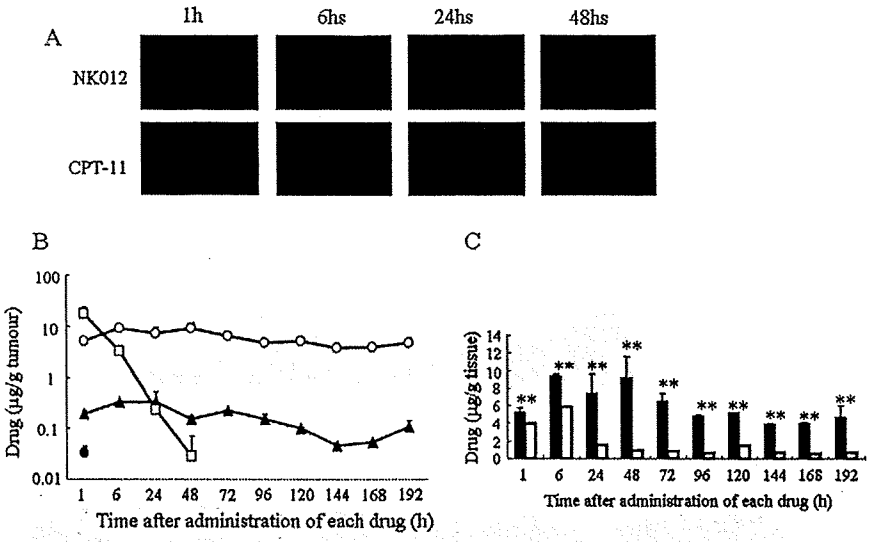

Fig. 4 – Distribution of NK012 or CPT-11 in orthotopic tumour xenografts. Concentrations of NK012 (polymer-bounded SN-38), free SN-38 and CPT-11 in tumour or normal pancreatic tissues. (A) Mice bearing SUIT-2 tumours were injected with NK012 (30 mg/kg) or CPT-11 (66.7 mg/kg). Tumour tissues were excised 1, 6, 24 and 48 h after intravenous NK012 or CPT-11. Each mouse was administered with fluorescein-labelled *Lycopersicon esculentum* lectin 5 min before sacrifice to detect tumour blood vessels. Frozen tissue sections were examined under a fluorescence microscope at an excitation wavelength of 377 nm and an emission wavelength of 477 nm. The same fluorescence condition can be applied for visualising NK012 and CPT-11 fluorescence. Scale bar, 100 μm. (B) Concentration of NK012 (polymer-bounded SN-38) (○), free SN-38 released from NK012 (▲), CPT-11 (□) and free SN-38 converted from CPT-11 (●) in orthotopic tumour xenografts. Points, mean + SD. (C) Concentration of NK012 (polymer-bounded SN-38) in tumour tissue or normal pancreatic tissue. Black column, tumour tissues, mean; white column, normal pancreatic tissue, mean. Bar, SD. **P < 0.01 (tumour tissue versus normal pancreas, each time).

of hypovascular tumours. A phase I clinical trial of NK012 has been completed.[26,27] A future phase II clinical trial in patients with hypovascular and stroma-rich tumour such as pancreatic cancer is warranted.

Conflict of interest statement

None declared.

Acknowledgements

The authors declared no potential conflict of interest. This work was supported partly by a Grant-in-Aid from the Third Term Comprehensive Control Research for Cancer, the Ministry of Health, Labour and Welfare (Matsumura, H19-025), Scientific Research on Priority Areas from the Ministry of Education, Culture, Sports, Science and Technology (Matsumura, 17016087), and Japanese Foundation for Multidisciplinary Treatment of Cancer (Matsumura) and the Princess Takamatsu Cancer Research Fund (07-23908). We thank N. Mie, M. Ohtsu and Y. Hashimoto for their technical assistance and K. Shiina for her secretarial assistance.

REFERENCES

1. Jemal A, Siegel R, Ward E, et al. Cancer statistics, 2008. *CA Cancer J Clin* 2008;58:71–96.
2. Warshaw AL, Fernández-del Castillo C. Pancreatic carcinoma. *N Engl J Med* 1992;326:455–65.
3. Wanebo HJ, Vezeridis MP. Pancreatic carcinoma in perspective. A continuing challenge. *Cancer* 1996;78:580–91.
4. Casper ES, Green MR, Kelsen DP, et al. Phase II trial of gemcitabine (2,2′-difluorodeoxycytidine) in patients with adenocarcinoma of the pancreas. *Invest New Drugs* 1994;12:29–34.
5. Carmichael J, Fink U, Russell RC, et al. Phase II study of gemcitabine in patients with advanced pancreatic cancer. *Br J Cancer* 1996;73:101–5.
6. Moore MJ, Goldstein D, Hamm J, et al. Erlotinib plus gemcitabine compared with gemcitabine alone in patients with advanced pancreatic cancer: a phase III trial of the National Cancer Institute of Canada Clinical Trials Group. *J Clin Oncol* 2007;25:1960–6.
7. Hosoki T. Dynamic CT of pancreatic tumors. *AJR Am J Roentgenol* 1983;140:959–65.
8. Sofuni A, Iijima H, Moriyasu F, et al. Differential diagnosis of pancreatic tumors using ultrasound contrast imaging. *J Gastroenterol* 2005;40:518–25.
9. Matsumura Y, Maeda H. A new concept for macromolecular therapeutics in cancer chemotherapy: mechanism of tumoritropic accumulation of proteins and the antitumor agent smancs. *Cancer Res* 1986;46:6387–92.
10. Li LH, Fraser TJ, Olin EJ, Bhuyan BK. Action of camptothecin on mammalian cells in culture. *Cancer Res* 1972;32:2643–50.
11. Gallo RC, Whang-Peng J, Adamson RH. Studies on the antitumor activity, mechanism of action, and cell cycle effects of camptothecin. *J Natl Cancer Inst* 1971;46:789–95.
12. Gottlieb JA, Guarino AM, Call JB, Oliverio VT, Block JB. Preliminary pharmacologic and clinical evaluation of camptothecin sodium (NSC-100880). *Cancer Chemother Rep* 1970;54:461–70.

13. Muggia FM, Creaven PJ, Hansen HH, Cohen MH, Selawry OS. Phase I clinical trial of weekly and daily treatment with camptothecin (NSC-100880): correlation with preclinical studies. *Cancer Chemother Rep* 1972;56:515–21.
14. Koizumi F, Kitagawa M, Negishi T, et al. Novel SN-38-incorporating polymeric micelles, NK012, eradicate vascular endothelial growth factor-secreting bulky tumors. *Cancer Res* 2006;66:10048–56.
15. Sumitomo M, Koizumi F, Asano T, et al. Novel SN-38-incorporated polymeric micelle, NK012, strongly suppresses renal cancer progression. *Cancer Res* 2008;68:1631–5.
16. Nakajima TE, Yasunaga M, Kano Y, et al. Synergistic antitumor activity of the novel SN-38-incorporating polymeric micelles, NK012, combined with 5-fluorouracil in a mouse model of colorectal cancer, as compared with that of irinotecan plus 5-fluorouracil. *Int J Cancer* 2008;122:2148–53.
17. Nakajima TE, Yanagihara K, Takigahira M, et al. Antitumor effect of SN-38-releasing polymeric micelles, NK012, on spontaneous peritoneal metastases from orthotopic gastric cancer in mice compared with irinotecan. *Cancer Res* 2008;68:9318–22.
18. Kuroda JI, Kuratsu JI, Yasunaga M, Koga Y, Saito Y, Matsumura Y. Potent antitumor effect of SN-38-incorporating polymeric micelle, NK012, against malignant glioma. *Int J Cancer* 2009;124:2505–11.
19. Saito Y, Yasunaga M, Kuroda J, Koga Y, Matsumura Y. Enhanced distribution of NK012, a polymeric micelle-encapsulated SN-38, and sustained release of SN-38 within tumors can beat a hypovascular tumor. *Cancer Sci* 2008;99:1258–64.
20. Koppe MJ, Oyen WJ, Bleichrodt RP, Verhofstad AA, Goldenberg DM, Boerman OC. Combination therapy using gemcitabine and radioimmunotherapy in nude mice with small peritoneal metastases of colonic origin. *Cancer Biother Radiopharm* 2006;21:506–14.
21. Yang HM, Reisfeld RA. Doxorubicin conjugated with a monoclonal antibody directed to a human melanoma-associated proteoglycan suppresses the growth of established tumor xenografts in nude mice. *Proc Natl Acad Sci USA* 1988;85:1189–93.
22. Kawato Y, Aonuma M, Hirota Y, Kuga H, Sato K. Intracellular roles of SN-38, a metabolite of the camptothecin derivative CPT-11, in the antitumor effect of CPT-11. *Cancer Res* 1991;51:4187–91.
23. Muggia FM. Liposomal encapsulated anthracyclines: new therapeutic horizons. *Curr Oncol Rep* 2001;3:156–62.
24. Hassan M, Little RF, Vogel A, et al. Quantitative assessment of tumor vasculature and response to therapy in kaposi's sarcoma using functional noninvasive imaging. *Technol Cancer Res Treat* 2004;3:451–7.
25. Emoto M, Udo T, Obama H, Eguchi F, Hachisuga T, Kawarabayashi T. The blood flow characteristics in borderline ovarian tumors based on both color Doppler ultrasound and histopathological analyses. *Gynecol Oncol* 1998;70:351–7.
26. Kato K, Hamaguchi T, Shirao K et al. Interim analysis of phase I study of NK012, polymer micelle SN-38, in patients with advanced cancer. *Proc Am Soc Clin Oncol GI 2008* [Abs #485].
27. Burris HA III, Infante JR, Spigel DR, et al. A phase I dose-escalation study of NK012. *Proc Am Soc Clin Oncol 2008* [Abs #2358].

Please cite this article in press as: Saito Y et al., Antitumour activity of NK012, SN-38-incorporating polymeric micelles, in hypovascular orthotopic pancreatic tumour, *Eur J Cancer* (2009), doi:10.1016/j.ejca.2009.11.014

UICC
global cancer control

IJC
International Journal of Cancer

Synergistic antitumor activity of the SN-38-incorporating polymeric micelles NK012 with S-1 in a mouse model of non-small cell lung cancer

Tatsuya Nagano[1,2,3], Masahiro Yasunaga[1], Koichi Goto[2], Hirotsugu Kenmotsu[2], Yoshikatsu Koga[1], Jun-ichiro Kuroda[1], Yoshihiro Nishimura[3], Takashi Sugino[4], Yutaka Nishiwaki[2] and Yasuhiro Matsumura[1]

[1] Investigative Treatment Division, Research Center for Innovative Oncology, National Cancer Center Hospital East, 6-5-1 Kashiwanoha, Kashiwa, Chiba, Japan

[2] Thoracic Oncology Division, National Cancer Center Hospital East, 6-5-1 Kashiwanoha, Kashiwa, Chiba, Japan

[3] Division of Respiratory Medicine, Department of Internal Medicine, Kobe University Graduate School of Medicine, 7-5-1 Kusunokicho, Chuo-ku, Kobe, Hyogo, Japan

[4] Department of Pathology, Fukushima Medical University School of Medicine, 1 Hikariga-oka, Fukushima, Fukushima, Japan

The combination therapy of CPT-11, a prodrug of SN-38, with S-1, a dihydropyrimidine dehydrogenase inhibitory fluoropyrimidine, shows a high clinical response rate in non-small cell lung cancer (NSCLC). However, this combination causes severe toxicities such as diarrhea. Here, we investigated the advantages of treatment with the SN-38-incorporating polymeric micelles NK012 over CPT-11 in combination with S-1 in mice bearing a NSCLC xenograft in terms of antitumor activity and toxic effects, particularly intestinal toxicity. *In vitro* cytotoxic effects were examined in human NSCLC cell lines (A549, PC-9, PC-14, EBC-1 and H520). *In vivo* antitumor effects were evaluated in PC-14- and EBC-1-bearing mice after NK012 or CPT-11 administration on Days 0 and 7 and S-1 administration on Days 0–13. Pathological changes in the small intestine were also investigated. The *in vitro* growth inhibitory effects of NK012 were 56.8- to 622-fold more potent than those of CPT-11. NK012/S-1 treatment showed significantly higher antitumor activity both in PC-14-bearing ($p = 0.0007$) and EBC-1-bearing mice ($p < 0.0001$) than CPT-11/S-1 treatment. The deformity and decrease in the density of intestinal villi were more severe in CPT-11/S-1-treated mice than in NK012/S-1-treated mice. NK012/S-1 combination is a promising candidate regimen against NSCLC without inducing toxicities such as severe diarrhea and therefore warrants clinical evaluation.

Lung cancer is the leading cause of death from malignancies worldwide in both men and women,[1] and accounted for 31% (male) and 26% (female) of all cancer deaths in 2008.[2] It is histologically classified into small-cell lung cancer (SCLC) and non-small cell lung cancer (NSCLC). The standard first-line chemotherapy for NSCLC is platinum-based regimens.[3] However, as shown in a randomized phase III study, the response rate to these regimens is only 30–33% and the 1-year survival rate is 48–59%, with a median survival period of 11–14 months for advanced NSCLC patients with PS 0 or 1.[4] Therefore, the development of new chemotherapeutic agents and combination regimens against NSCLC is urgently desired.

Irinotecan hydrochloride (CPT-11), an anticancer drug, is converted to its biologically active metabolite 7-ethyl-10-hydroxy-camptothecin (SN-38) by carboxylesterases, and SN-38 has been shown to be efficacious against various human cancers such as colorectal, lung and ovarian cancer.[5–8] Although SN-38 has 1,000-fold more potent cytotoxic activity against various cancer cell lines *in vitro* than CPT-11,[9] its conversion rate from CPT-11 to SN-38 is <10% of the original CPT-11 dose in the body.[10,11]

On the other hand, the SN-38-incorporating polymeric micelles NK012 appear to have the advantage of passive targeting of the drug delivery system (DDS). In this passive DDS targeting, the drug accumulates in tumor tissue by utilizing the enhanced permeability and retention (EPR) effect.[12–15] This EPR effect is based on several pathological mechanisms that include hypervascularity, secretion of tumor vascular permeability factors stimulating extravasation of macromolecules including nanoparticles such as liposomes and micelles, and the absence of an effective lymphatic

Key words: NK012, S-1, diarrhea, drug delivery system, non-small cell lung cancer

Grant sponsor: Ministry of Education, Culture, Sports, Science and Technology (Scientific Research on Priority Areas); **Grant number:** 17016087; **Grant sponsors:** Third Term Comprehensive Control Research for Cancer, Japanese Foundation for Multidisciplinary Treatment of Cancer, Ministry of Health, Labor and Welfare; **Grant number:** H19-025

DOI: 10.1002/ijc.25282

History: Received 18 Dec 2009; Accepted 26 Jan 2010; Online 2 Mar 2010

Correspondence to: Yasuhiro Matsumura, Investigative Treatment Division, Research Center for Innovative Oncology, National Cancer Center Hospital East, 6-5-1 Kashiwanoha, Kashiwa, Chiba 277-8577, Japan, Tel.: +81-(0)-4-7133-1111(Ex: 5400), Fax: +81-(0)-4-7134-6866, E-mail: yhmatsum@east.ncc.go.jp

drainage of macromolecules accumulated in solid tumor tissue. In the previous study, we evaluated the antitumor effect by histopathologic evaluation and immunohistochemistry and demonstrated decreased cellularity, increased tumor stroma, and inflammatory cell infiltrations in the tumors treated with NK012. Tumors treated with CPT-11 showed no apparent morphologic differences from control tumors. Concordant with morphologic changes, the number of Ki-67 tumor cells tended to decrease in tumors treated with NK012 compared with CPT-11.[16] Recent studies demonstrated that NK012 is significantly more potent than CPT-11 against SCLC,[17] colorectal cancer,[18] renal cancer,[19] pancreatic cancer,[20] stomach cancer[21] and glioma.[22] Furthermore, in 2 independent phase I clinical trials in Japan[23] and the US,[24] nonhematological toxicities were minimal and grade 3/4 diarrhea, a major clinically important toxic effect or dose-limiting factor of CPT-11, was absent.

CPT-11 causes cell accumulation in the S phase, and 5-fluorouracil (5-FU) infusion induces DNA damage specifically in cells in the S phase.[25] Moreover, CPT-11 reduces thymidylate synthase (TS) and dihydropyrimidine dehydrogenase (DPD) mRNA expression,[26] and low gene expression level of TS and DPD had association with the response rate or chemosensitivity to 5-FU in metastatic colorectal cancer.[27,28] Recently, we demonstrated the higher synergistic antitumor activity of the NK012/5-FU combination against a colorectal tumor xenograft than the CPT-11/5-FU combination.[18] However, the use of an indwelling central venous catheter and a portable pump for 5-FU infusion may cause infection or thrombosis, and incur higher healthcare costs.[29]

S-1, on the other hand, is an oral anticancer agent composed of a 5-FU prodrug (tegafur), 5-chloro-2, 4-dihydroxypyrimidine (CDHP), and potassium oxonate (molar ratio = 1:0.4:1) and is categorized under DPD inhibitory fluoropyrimidines.[30] Tegafur generates 5-FU in the blood primarily *via* metabolism by liver enzyme cytochrome P450. CDHP enhances the serum 5-FU concentration by inhibiting the DPD activity competitively. Potassium oxonate is a reversible competitive inhibitor of orotate phosphoribosyl transferase, a phosphoenzyme for 5-FU and attributes to phosphorylation of 5-FU in the gastrointestinal tract and is expected to reduce the intestinal toxicity that is one of the clinical problems of 5-FU.[31]

In this context, we investigated the advantages of NK012/S-1 over CPT-11/S-1 in mice bearing a NSCLC xenograft in terms of antitumor activity and toxic effects, particularly intestinal toxicity.

Material and Methods

Drugs and cells

SN-38 and NK012 were prepared by Nippon Kayaku Co., (Tokyo, Japan). CPT-11 was purchased from Yakult Honsha Co., (Tokyo, Japan). S-1 was obtained from Taiho Pharmaceutical Co. (Tokyo, Japan). 5-FU was purchased from Kyowa Hakko (Tokyo, Japan).

The NSCLC cell lines A549, PC-9, PC-14, EBC-1 and H520 were purchased from the American Type Culture Collection (Rockville, MD). They were maintained in RPMI-1640 supplemented with 10% fetal bovine serum (Cell Culture Technologies, Gaggenau-Hoerden, Germany), penicillin, streptomycin and amphotericin B (100 units/mL, 100 μg/mL and 25 μg/mL, respectively; Sigma, St. Louis, MO) in a humidified atmosphere containing 5% CO_2 at 37°C.

In vitro growth inhibition assay

The growth inhibitory effects of NK012, CPT-11, SN-38 and 5-FU, instead of S-1 that is not suitable for use *in vitro*, because tegafur is a prodrug that is mainly activated in liver were examined by tetrazolum salt-based proliferation assay (WST-8 assay; Wako Chemicals, Osaka, Japan). A suspension (100 mL) of exponentially growing cells (1×10^5/mL) was placed into the wells of a 96-well plate and incubated for 24 hr at 37°C. Following medium removal, 100 μL of medium containing various concentrations of each drug was added to the wells and then incubated for 72 hr at 37°C. After medium removal, 10 μL of WST-8 solution and 90 μL of medium were added to the wells, followed by incubation for 1 hr at 37°C. The growth inhibitory effects of each drug were assessed spectrophotometrically (SpectraMax 190, Molecular Devices Corp., Sunnyvale, CA). IC_{50} was determined on the dose–response curves. The nature of interaction between NK012 and 5-FU against the NSCLC cell lines A549, PC-9, PC-14, EBC-1 and H520 was evaluated by median-effect plot analyses and the combination index method of Chou and Talalay.[32]

Reverse transcription and real-time PCR analysis

A suspension (2 mL) of exponentially growing cells (1×10^5/mL) was placed into the wells of a 6-well plate and incubated for 24 hr at 37°C. Following medium removal, 2 mL of medium and medium containing NK012 (1 μM) and CPT-11 (1 μM) were added to the wells and then incubated for 24 hr at 37°C ($n = 3$ for each arm), as reported.[33] Total RNA (1 μg) extracted from cells using an RNeasy Mini kit (Qiagen, Valencia, CA) was subjected to reverse transcription using the High Capacity cDNA Reverse Transcription kit (Applied Biosystems, Foster, CA). The resulting cDNA was then subjected to real-time PCR analysis using a Taqman PCR Reagent kit and an Applied Biosystems 7500 Fast Real-Time PCR System (Applied Biosystems). To quantify TS and DPD, we used TaqMan primers and a probe mixture (Applied Biosystems). Glyceraldehyde-3-phosphate dehydrogenase (GAPDH) mRNA was used as an internal control. Relative quantification of the total RNA in each sample was conducted using the comparative Ct (threshold cycle) method. The formulae for the relative quantification of each gene were as follows: (dCt of each gene) = (Ct of each gene) − (Ct of GAPDH), and (Relative quantification of each gene) = $2^{-(\text{dCt of each gene})}$.

Table 1. *In vitro* growth inhibitory activity of SN-38, NK012, CPT-11 and 5-FU in human non-small cell lung cancer cells

	IC50 (μmol/L)			
Cell line	SN-38	NK012	CPT-11	5-FU
A549	0.500 ± 0.092	0.888 ± 0.096	50.4 ± 2.3	419 ± 44
PC-9	0.0574 ± 0.0414	0.0732 ± 0.0020	8.86 ± 0.43	15.0 ± 4.2
PC-14	0.0488 ± 0.0011	0.0554 ± 0.0118	7.53 ± 4.97	2.99 ± 0.27
EBC-1	0.00374 ± 0.00449	0.00747 ± 0.00053	4.65 ± 0.17	45.8 ± 2.6
H520	0.0721 ± 0.0131	0.0773 ± 0.0071	9.10 ± 0.29	13.6 ± 7.1

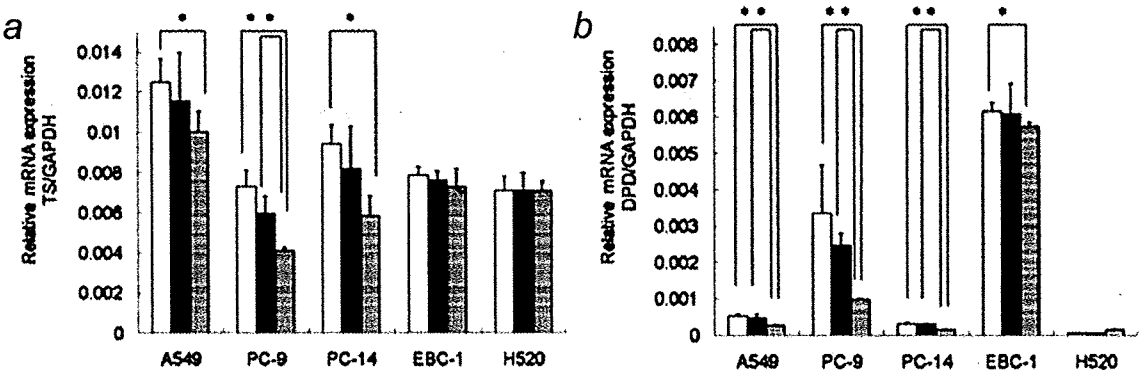

Figure 1. Effects of NK012 and CPT-11 on the expression of TS and DPD mRNA in non-small cell lung cancer (NSCLC) cell lines. (*a, b*) Downregulation of TS (*a*) and DPD (*b*) mRNA by NK012 and CPT-11 in NSCLC cell lines. A549, PC-9, PC-14, EBC-1 and H520 cells were incubated with medium containing 10% serum, medium containing NK012 (1 μmol/L) and 10% serum, and medium containing CPT-11 (1 μmol/L) and 10% serum for 24 hr. Then, total RNA was extracted from the cells and subjected to reverse transcription and real-time PCR analysis of TS and DPD mRNA. The amount of TS and DPD mRNA was normalized to that of glyceraldehyde-3-phosphate dehydrogenase mRNA. Bars, SD. *, $p < 0.05$. □, Medium; ■, CPT-11; ⊟, NK012.

Experimental mice model

Female BALB/c nude mice (6-weeks-old) were purchased from SLC Japan (Shizuoka, Japan). Mice were inoculated subcutaneously in the flank with 2.5×10^6 cells/50 μL cell suspension of PC-14 and 1.0×10^6 cells/50 μL cell suspension of EBC-1.

All animal procedures were performed in compliance with the guidelines for the care and use of experimental animals established by the Committee for Animal Experimentation of the National Cancer Center. These guidelines meet the ethical standards required by law and comply with the guidelines for the use of experimental animals in Japan.

In vivo growth inhibition assay

When the tumor volume (TV) reached 250 mm^3, mice were randomly divided into test groups consisting of 5 mice per group (Day 0). NK012, CPT-11, or NaCl solution (0.9%) was intravenously (i.v.) administered into the tail vein on Days 0 and 7. NK012 was administered at 5 mg/kg/d, which is 1/6 of the maximum tolerated dose (MTD). CPT-11 (reference drug) was administered at 10 mg/kg/d, which is also 1/6 of the MTD. S-1 was singularly or simultaneously administered by oral gavage once a day on Days 0–13 at 10 mg/kg/d, as reported.[34] NaCl solution (0.9%) was administered i.v. as normal control. The length (*a*) and width (*b*) of the tumor masses and body weight (BW) were measured twice a week, and TV was calculated using $TV = (a \times b^2)/2$. Relative tumor volume (RTV) on day n was calculated using $RTV = TV_n/TV_0$, where TV_n is the tumor volume on Day n and TV_0 is the tumor volume on Day 0. Relative body weight (RBW) was calculated using $RBW = BW_n/BW_0$. We evaluated the feces of mice on Days 4, 11 and 18 and considered soft, wet and canescent feces to indicate diarrhea, as reported.[35]

Experiment 1. Evaluation of the synergistic effects of NK012 with S-1. NK012, S-1, NK012/S-1, or NaCl solution (0.9%) was administered following the above dose schedules. We evaluated the effects of NK012/S-1 by comparing the data between NK012/S-1 and the additive effect (expected RTV). Expected RTV was calculated using (RTV of NK012) × (RTV of S-1) / (RTV of control), as reported.[36]

Experiment 2. Comparison of the antitumor effects of NK012/S-1 and CPT-11/S-1. NK012/S-1, CPT-11/S-1, or NaCl solution (0.9%) was administered following the above dose schedules. Two-way analysis of variance (ANOVA) was performed to compare the transitional RTV between NK012/S-1-treated mice and CPT-11/S-1-treated mice.

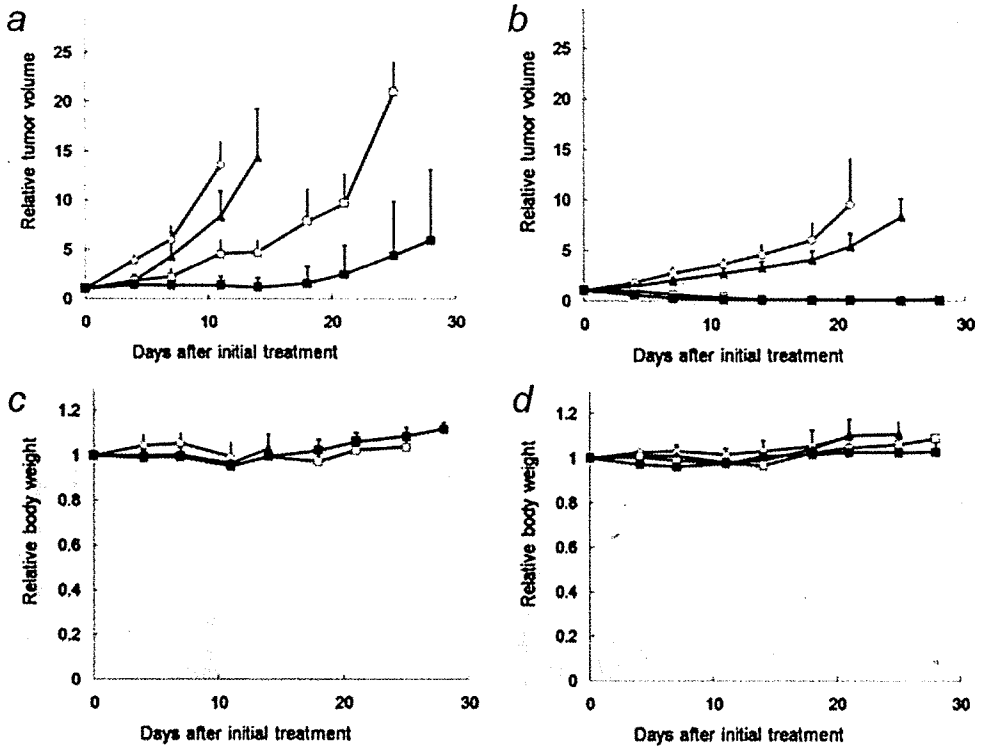

Figure 2. Growth inhibitory effects of NK012, S-1 and NK012/S-1 on PC-14 and EBC-1 tumor xenografts. (*a*, *b*) Relative tumor volume in mice treated with NK012, S-1 and NK012/S-1. PC-14 (*a*, *c*) and EBC-1 (*b*, *d*) cells were inoculated subcutaneously into the flank of mice, as described in Material and Methods. Drug administration was as follows: NK012 (5 mg/kg/d) on Days 0 and 7 (□), S-1 (10 mg/kg/d) on Days 0–13 (▲), NK012 (5 mg/kg/d) on Days 0 and 7 and combined with S-1 (10 mg/kg/d) on Days 0–13 (■), or NaCl solution (0.9%) on Days 0 and 7 as normal control (○). Points, mean; bars, SD. *, $p < 0.05$. (*c*, *d*) Treatment-related body weight loss occurred in mice treated with each drug. Points, mean; bars, SD.

Pathological studies of small intestinal mucosa

NaCl solution, CPT-11, NK012, S-1, CPT-11/S-1 and NK012/S-1 were administered to female BALB/c nude mice ($n = 3$) following the same dose schedules as those used in the treatment experiment. On Day 7 after the last dozing, mice were sacrificed and the small intestine was sampled at the middle portion. Samples were fixed in 10% formalin, paraffin-embedded, sectioned and stained with H&E. Villi density was defined as the number of villi per mm. We also evaluated the fecal condition mice on Days 4, 11 and 18. The extent of diarrhea as well as the appearance and number of villi was scored by independent, 2 blinded researchers.

Statistical analysis

Data were analyzed with Student's *t*-test when groups showed equal variances (*F* test) or Welch's test when they showed unequal variances (*F* test). ANOVA was performed to compare transitional RTV. Differences in the number of mice with diarrhea between NK012/S-1-treated mice and CPT-11/S-1-treated mice were tested for significance using the Pearson χ^2 test or Fisher exact test. All analyses were performed using StatView 5.0, and $p < 0.05$ was considered significant. All statistical tests were 2 sided, and data were expressed as mean ± SD.

Results

Sensitivity of NSCLC cells to NK012, CPT-11, SN-38 and S-1

The IC_{50} values of NK012 for the NSCLC cell lines ranged from 0.00747 μmol/L (EBC-1) to 0.888 μmol/L (A549) (Table 1). The cytotoxic effects of NK012 were 56.8- to 622-fold higher than those of CPT-11, whereas those of NK012 were 1.07- to 2.00-fold lower than those of SN-38. These features were comparable to those reported previously.[17,37] The molar ratios of NK012: 5-FU of 1:500 in A549, 1:200 in PC-9 and H520, 1:50 in PC-14, and 1:6,000 in EBC-1 were used for the drug combination studies based on the IC_{50} values of NK012 and 5-FU (Table 1). The synergic to additive effect between NK012 and 5-FU was observed in these NSCLC cell lines (data not shown).

Effects of NK012 and CPT-11 on the expression of TS and DPD mRNA in NSCLC cell lines

NK012 induced a significant decrease in TS mRNA expression in A549, PC-9 and PC-14 ($p = 0.0487$, $p = 0.0027$ and $p = 0.0095$, respectively) compared with the control, as well as in PC-9 ($p = 0.0225$) compared with CPT-11. NK012 also tended to decrease TS mRNA expression in EBC-1 and H520 compared with the control and CPT-11 (Fig. 1*a*). NK012

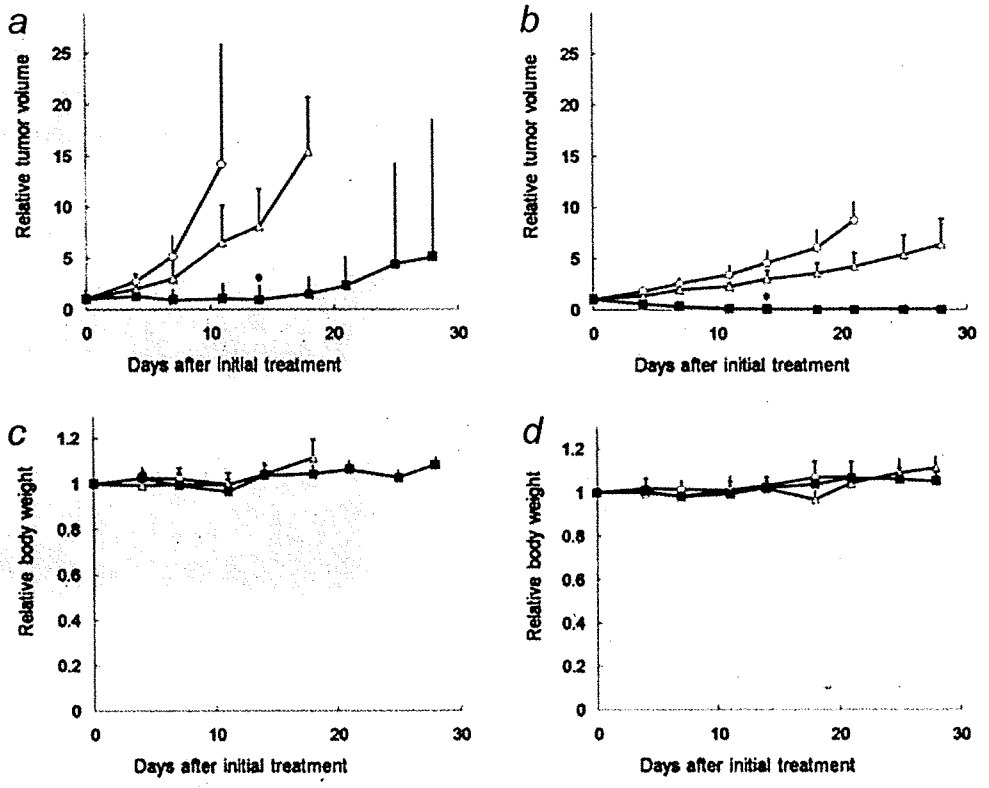

Figure 3. Antitumor effect of combined NK012/S-1 and CPT-11/S-1 treatment on PC-14 and EBC-1 tumor xenografts. (*a*, *b*) Relative tumor volume in mice treated with NK012/S-1 or CPT-11/S-1. PC-14 (*a*, *c*) and EBC-1 (*b*, *d*) cells were inoculated subcutaneously into the flank of mice, as described in Material and Methods. Drug administration was as follows: NK012 (5 mg/kg/d) on Days 0 and 7 and combined with S-1 (10 mg/kg/d) on Days 0–13 (■), CPT-11 (10 mg/kg/d) on Days 0 and 7 and combined with S-1 (10 mg/kg/d) on Days 0–13 (△), or NaCl solution (0.9%) on Days 0 and 7 as normal control (○). Points, mean; bars, SD. *, $p < 0.05$. (*c*, *d*) Treatment-related body weight loss occurred in each treated-mouse. Points, mean; bars, SD.

Table 2. Diarrhea after i.v. administrations of drugs

	Control	S-1	NK012	S-1 + NK012	CPT-11	S-1 + CPT-11
Day 4	0/24 (0)	1/13 (7.7)	0/10 (0)	1/24 (4.2)	0/4 (0)	3/14 (21.4)
Day 11	0/24 (0)	2/13 (15.4)	0/10 (0)	6/24 (25)	0/4 (0)	7/14 (50.0)
Day 18	0/24 (0)	0/13 (0)	0/10 (0)	2/24 (8.3)	0/4 (0)	3/14 (21.4)

Values in parentheses indicate percentage.

induced a significant decrease in DPD mRNA expression in A549, PC-9, PC-14 and EBC-1 ($p = 0.0019$, $p = 0.0358$, $p = 0.0020$ and $p = 0.0399$, respectively) compared with the control, as well as in A549, PC-9 and PC-14 ($p = 0.0373$, $p = 0.0013$ and $p = 0.0001$, respectively) compared with CPT-11. NK012 also tended to decrease DPD mRNA expression in EBC-1 compared with CPT-11, but not in H520 (Fig. 1*b*).

Antitumor activity of S-1, NK012, NK012/S-1, CPT-11 and CPT-11/S-1 against PC-14 and EBC-1 tumors

The therapeutic effect of NK012/S-1 was significantly superior to that of NK012 both in PC-14 ($p = 0.0013$) (Fig. 2*a*) and EBC-1 ($p = 0.0017$) (Fig. 2*b*), and this combination demonstrated a synergistic efficacy. The complete response rates achieved with NK012 and NK012/S-1 were 0 and 20% for PC-14 and 40 and 100% for EBC-1, respectively. Although treatment-related BW loss was observed in mice treated with each drug combination, BW recovered to the normal level in each group by Day 21 (Figs. 2*c* and 2*d*).

The therapeutic effect of NK012/S-1 was significantly superior to that of CPT-11/S-1 in PC-14-bearing ($p = 0.0007$) (Fig. 3*a*) and EBC-1-bearing mice ($p < 0.0001$) (Fig. 3*b*). The complete response rates achieved with NK012/S-1 were 40 and 100% for PC-14 and EBC-1, respectively. Although slight treatment-related BW loss was observed in mice treated with each drug combination, there was no significant difference between NK012/S-1 and CPT-11/S-1, and BW recovered to the normal level in each group by Day 21 (Figs. 3*c* and 3*d*).

Intestinal toxicity of CPT-11, NK012, S-1, CPT-11/S-1 and NK012/S-1

The mice treated with NaCl solution (0.9%), CPT-11, and NK012 had no diarrhea, whereas those treated with S-1, CPT-11/S-1 and NK012/S-1 had diarrhea (Table 2). The mice treated with CPT-11/S-1 tended to have higher incidence of diarrhea than those treated with S-1 ($p = 0.596$ Day 4, $p = 0.103$ Day 11, and $p = 0.222$ Day 18) or NK012/S-1 ($p = 0.132$ Day 4, $p = 0.163$ Day 11, and $p = 0.337$ Day 18).

The small intestinal mucosa of mice on Day 7 after the last treatment with NaCl solution (0.9%), CPT-11, and NK012 showed regular alignment of normal villi (Fig. 4). On the other hand, the small intestinal mucosa of mice treated with S-1, CPT-11/S-1 and NK012/S-1 showed deformation of villi, specifically a decrease in height and width. In particular, mice treated with CPT-11/S-1 showed more severe deformation and decrease in height and width of villi, as well as a more severe decrease in villi density than those treated with S-1 and NK012/S-1. Furthermore, CPT-11/S-1 treatment decreased villi density the most under the microscopic observation (Fig. 4*b*).

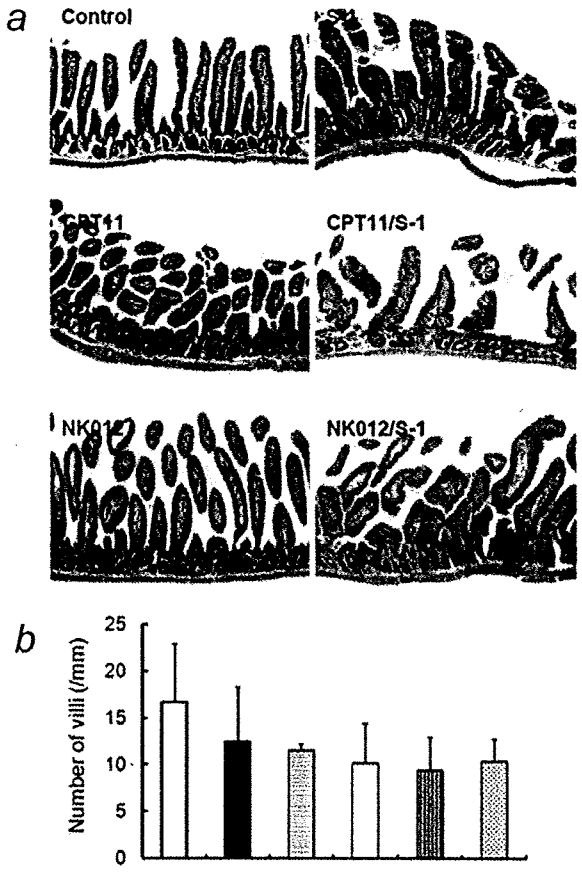

Figure 4. Pathological findings in intestinal mucosa. Mice were administered the following: NaCl solution (0.9%) on Days 0 and 7 as normal control, CPT-11 (10 mg/kg/d) on Days 0 and 7, NK012 (5 mg/kg/d) on Days 0 and 7, S-1 (10 mg/kg/d) on Days 0–13, CPT-11 (10 mg/kg/d) on Days 0 and 7 and combined with S-1 (10 mg/kg/d) on Days 0–13, or NK012 (5 mg/kg/d) on Days 0 and 7 and combined with S-1 (10 mg/kg/d) on Days 0–13. (*a*) Mice were sacrificed on Day 21 and the small intestine was sampled at the middle portion. Samples were fixed in 10% formalin, paraffin-embedded, sectioned and stained with H&E. In the NaCl-, CPT-11- and NK012-treated mice, the small intestinal mucosa showed regular alignment of normal villi. In the S-1- and NK012/S-1-treated mice, the small intestinal mucosa showed deformation of villi, specifically decreased height and width. This was also observed in CPT-11/S-1-treated mice with accompanying severe decrease in villi density. (*b*) Villi density indicates the number of villi per mm. Villi density was decreased the most with CPT-11/S-1 treatment. □, NaCl solution; ■, CPT-11; ⊟, NK012; ⊡, S-1; ◫, CPT-11/S-1; ▨, NK012 /S-1.

Discussion

The present study showed the synergistic effect between NK012 and S-1 and the significant antitumor activity of NK012/S-1 compared with CPT-11/S-1, the latter being one of the promising combinations against several cancers including NSCLC.[38] Indeed, CPT-11 combined with S-1 also exhibits potentially promising clinical activity with favorable toxic profile not only in NSCLC, but also advanced colorectal cancer,[29] and metastatic advanced gastric cancer.[39] Previously, we studied the differences in the effects between NK012 and CPT-11 on the cell cycle and demonstrated that NK012 induced a more prolonged accumulation of tumor cells in the S phase than CPT-11,[18] and this may explain the higher synergistic effect of NK012/5-FU than CPT-11/5-FU. Here, NK012 caused a larger decrease in TS and DPD mRNA expression than CPT-11. TS and DPD mRNA is thought to be associated with fluoropyrimidine sensitivity in lung cancer,[40] and a greater synergistic effect is expected between NK012 and fluoropyrimidines than between CPT-11 and fluoropyrimidines. In a phase II study of CPT-11/S-1 for advanced NSCLC, the grade 3/4 hematologic toxicities observed included neutropenia (25%), thrombocytopenia (3.6%) and anemia (3.6%), and the most common grade 3/4 nonhematologic toxicities were anorexia (14.3%), fatigue (8.9%) and diarrhea (8.9%).[38] Severe late-onset diarrhea is a major clinically important toxic effect or dose-limiting factor of CPT-11.[41–43] Diarrhea is also a clinical problem in S-1 treatment.[44] We previously demonstrated that a large amount of CPT-11 was excreted into the feces and high CPT-11 concentration was detected in the small intestinal epithelium. In contrast, a small amount of NK012 was found in the feces and NK012 was weakly and uniformly distributed in the mucosal interstitium. Furthermore, inflammatory changes in the small intestinal mucosa were rare in all NK012-treated mice, but were commonly observed in CPT-11-treated mice.[45] Here, in the present study, we used the same nude mice bearing human tumor xenografts in order to compare the present data with the previous data and demonstrated CPT-11/S-1 treatment induced more severe deformation of villi,

specifically decreased height and width, and severe decrease in villi density than NK012/S-1. Furthermore, villi density in CPT-11/S-1-treated mice was less than that in NK012/S-1-treated mice. The incidence of CPT-11/S-1-induced diarrhea was higher than that of NK012/S-1-induced diarrhea, although the difference was not significant ($p = 0.132$–0.337). There was no significant difference in other toxic effects including bone marrow and liver toxicities between NK012/S-1 and CPT-11/S-1 in the present treatment schedule (data not shown).

In conclusion, NK012/S-1 showed a significantly higher antitumor activity with less intestinal damage than CPT-11/S-1, one of the promising regimens against NSCLC, advanced colorectal cancer and metastatic advanced gastric cancer. Phase II clinical trials of NK012 monotherapy are now underway in patients with colorectal cancer in Japan and patients with triple negative breast cancer or SCLC in the USA. The present results suggest the clinical evaluation of NK012/S-1 in NSCLC patients.

Acknowledgements

This work was supported partly by a Grant-in-Aid from the Third Term Comprehensive Control Research for Cancer, the Ministry of Health, Labor and Welfare (Goto, Nishiwaki, and Matsumura), Scientific Research on Priority Areas from the Ministry of Education, Culture, Sports, Science and Technology (Matsumura), and the Japanese Foundation for Multidisciplinary Treatment of Cancer (Matsumura). The authors thank Ms. N. Mie and Ms. M. Ohtsu for technical assistance and Ms. K. Shiina and Ms. K. Abe for secretarial assistance.

References

1. Spiro SG, Porter JC. Lung cancer—where are we today? Current advances in staging and nonsurgical treatment. *Am J Respir Crit Care Med* 2002;166:1166–96.
2. Jemal A, Siegel R, Ward E, Hao Y, Xu J, Murray T, Thun MJ. Cancer statistics, 2008. *CA Cancer J Clin* 2008;58:71–96.
3. Schiller JH, Harrington D, Belani CP, Langer C, Sandler A, Krook J, Zhu J, Johnson DH. Comparison of four chemotherapy regimens for advanced non-small-cell lung cancer. *N Engl J Med* 2002;346:92–8.
4. Ohe Y, Ohashi Y, Kubota K, Tamura T, Nakagawa K, Negoro S, Nishiwaki Y, Saijo N, Ariyoshi Y, Fukuoka M. Randomized phase III study of cisplatin plus irinotecan versus carboplatin plus paclitaxel, cisplatin plus gemcitabine, and cisplatin plus vinorelbine for advanced non-small-cell lung cancer: Four-Arm Cooperative Study in Japan. *Ann Oncol* 2007;18:317–23.
5. Argiris A, Murren JR. Advances in chemotherapy for small cell lung cancer: single-agent activity of newer agents. *Cancer J* 2001;7:228–35.
6. Bodurka DC, Levenback C, Wolf JK, Gano J, Wharton JT, Kavanagh JJ, Gershenson DM. Phase II trial of irinotecan in patients with metastatic epithelial ovarian cancer or peritoneal cancer. *J Clin Oncol* 2003;21:291–7.
7. Cunningham D, Pyrhonen S, James RD, Punt CJ, Hickish TF, Heikkila R, Johannesen TB, Starkhammar H, Topham CA, Awad L, Jacques C, Herait P. Randomised trial of irinotecan plus supportive care versus supportive care alone after fluorouracil failure for patients with metastatic colorectal cancer. *Lancet* 1998;352:1413–18.
8. Negoro S, Masuda N, Takada Y, Sugiura T, Kudoh S, Katakami N, Ariyoshi Y, Ohashi Y, Niitani H, Fukuoka M. Randomised phase III trial of irinotecan combined with cisplatin for advanced non-small-cell lung cancer. *Br J Cancer* 2003;88:335–41.
9. Mathijssen RH, van Alphen RJ, Verweij J, Loos WJ, Nooter K, Stoter G, Sparreboom A. Clinical pharmacokinetics and metabolism of irinotecan (CPT-11). *Clin Cancer Res* 2001;7:2182–94.
10. Rothenberg ML, Kuhn JG, Burris HA, III, Nelson J, Eckardt JR, Tristan-Morales M, Hilsenbeck SG, Weiss GR, Smith LS, Rodriguez GI, Rock MK, Von Holf DD. Phase I and pharmacokinetic trial of weekly CPT-11. *J Clin Oncol* 1993;11:2194–204.
11. Slatter JG, Schaaf LJ, Sams JP, Feenstra KL, Johnson MG, Bombardt PA, Cathcart KS, Verburg MT, Pearson LK, Compton LD, Miller LL, Baker DS, et al. Pharmacokinetics, metabolism, and excretion of irinotecan (CPT-11) following I.V. infusion of [(14)C]CPT-11 in cancer patients. *Drug Metab Dispos* 2000;28:423–33.
12. Dvorak HF, Nagy JA, Dvorak JT, Dvorak AM. Identification and characterization of the blood vessels of solid tumors that are leaky to circulating macromolecules. *Am J Pathol* 1988;133:95–109.
13. Maeda H, Matsumura Y. Tumoritropic and lymphotropic principles of macromolecular drugs. *Crit Rev Ther Drug Carrier Syst* 1989;6:193–210.
14. Matsumura Y, Maeda H. A new concept for macromolecular therapeutics in cancer chemotherapy: mechanism of tumoritropic accumulation of proteins and the antitumor agent smancs. *Cancer Res* 1986;46:6387–92.
15. Matsumura Y, Maruo K, Kimura M, Yamamoto T, Konno T, Maeda H: Kinin-generating cascade in advanced cancer patients and in vitro study. *Jpn J Cancer Res* 1991;82:732–41.
16. Kuroda J, Kuratsu J, Yasunaga M, Koga Y, Kenmotsu H, Sugino T, Matsumura Y. Antitumor effect of NK012, a 7-ethyl-10-hydroxycamptothecin-incorporating polymeric micelle, on U87MG orthotopic glioblastoma in mice compared with irinotecan hydrochloride in combination with bevacizumab. *Clin Cancer Res* 2010;16:521–9.
17. Koizumi F, Kitagawa M, Negishi T, Onda T, Matsumoto S, Hamaguchi T, Matsumura Y. Novel SN-38-incorporating polymeric micelles, NK012, eradicate vascular endothelial growth factor-secreting bulky tumors. *Cancer Res* 2006;66:10048–56.
18. Nakajima TE, Yasunaga M, Kano Y, Koizumi F, Kato K, Hamaguchi T, Yamada Y, Shirao K, Shimada Y, Matsumura Y. Synergistic antitumor activity of the novel SN-38-incorporating polymeric micelles, NK012, combined with 5-fluorouracil in a mouse model of colorectal cancer, as compared with that of irinotecan plus 5-fluorouracil. *Int J Cancer* 2008;122:2148–53.
19. Sumitomo M, Koizumi F, Asano T, Horiguchi A, Ito K, Asano T, Kakizoe T, Hayakawa M, Matsumura Y. Novel SN-38-incorporated polymeric micelle, NK012, strongly suppresses renal cancer progression. *Cancer Res* 2008;68:1631–5.
20. Saito Y, Yasunaga M, Kuroda J, Koga Y, Matsumura Y. Enhanced distribution of NK012, a polymeric micelle-encapsulated SN-38, and sustained release of SN-38 within tumors can beat a hypovascular tumor. *Cancer Sci* 2008;99:1258–64.
21. Eguchi Nakajima T, Yanagihara K, Takigahira M, Yasunaga M, Kato K, Hamaguchi T, Yamada Y, Shimada Y, Mihara K, Ochiya T, Matsumura Y. Antitumor effect of SN-38-releasing polymeric micelles, NK012, on spontaneous peritoneal metastases from orthotopic gastric cancer in mice compared with irinotecan. *Cancer Res* 2008;68:9318–22.

22. Kuroda J, Kuratsu J, Yasunaga M, Koga Y, Saito Y, Matsumura Y. Potent antitumor effect of SN-38-incorporating polymeric micelle, NK012, against malignant glioma. *Int J Cancer* 2009;124:2505–11
23. Kato K, Hamaguchi T, Shirao K, Shimada Y, Doi T, Ohtsu A, Matsumura Y, Yamada Y. Interim analysis of phase I study of NK012, polymer micelle SN-38, in patients with advanced cancer. *Proc Am Soc Clin Oncol* 2008 (Abstract No. 485).
24. Burris HA, III, Infante JR, Spigel DR, Greco FA, Thompson DS, Matsumoto S, Kawamura S, Jones SF. A phase I dose-escalation study of NK012. *Proc Am Soc Clin Oncol* 2008 (Abstract No. 2538).
25. Azrak RG, Cao S, Slocum HK, Toth K, Durrani FA, Yin MB, Pendyala L, Zhang W, McLeod HL, Rustum YM. Therapeutic synergy between irinotecan and 5-fluorouracil against human tumor xenografts. *Clin Cancer Res* 2004;10: 1121–9.
26. Takiuchi H, Kawabe S-i, Gotoh M, Katsu K-i. Thymidylate synthase gene expression in primary tumors predicts activity of S-1-based chemotherapy for advanced gastric cancer. *Gastrointest Cancer Res* 2007;1: 171–6.
27. Salonga D, Danenberg KD, Johnson M, Metzger R, Groshen S, Tsao-Wei DD, Lenz HJ, Leichman CG, Leichman L, Diasio RB, Danenberg PV. Colorectal tumors responding to 5-fluorouracil have low gene expression levels of dihydropyrimidine dehydrogenase, thymidylate synthase, and thymidine phosphorylase. *Clin Cancer Res* 2000;6:1322–7.
28. Metzger R, Danenberg K, Leichman CG, Salonga D, Schwartz EL, Wadler S, Lenz HJ, Groshen S, Leichman L, Danenberg PV. High basal level gene expression of thymidine phosphorylase (platelet-derived endothelial cell growth factor) in colorectal tumors is associated with nonresponse to 5-fluorouracil. *Clin Cancer Res* 1998;4: 2371–6.
29. Goto A, Yamada Y, Yasui H, Kato K, Hamaguchi T, Muro K, Shimada Y, Shirao K. Phase II study of combination therapy with S-1 and irinotecan in patients with advanced colorectal cancer. *Ann Oncol* 2006;17:968–73.
30. Shirasaka T, Shimamoto Y, Fukushima M. Inhibition by oxonic acid of gastrointestinal toxicity of 5-fluorouracil without loss of its antitumor activity in rats. *Cancer Res* 1993;53:4004–9.
31. Muraoka A, Suehiro I, Fujii M, Nagata K, Kusunoki H, Kumon Y, Shirasaka D, Hosooka T, Murakami K. Acute gastric anisakiasis: 28 cases during the last 10 years. *Dig Dis Sci* 1996;41:2362–5.
32. Chou TC, Talalay P. Quantitative analysis of dose-effect relationships: the combined effects of multiple drugs or enzyme inhibitors. *Adv Enzyme Regul* 1984;22: 27–55.
33. Kamiyama H, Takano S, Tsuboi K, Matsumura A. Anti-angiogenic effects of SN38 (active metabolite of irinotecan): inhibition of hypoxia-inducible factor 1 α (HIF-1α)/vascular endothelial growth factor (VEGF) expression of glioma and growth of endothelial cells. *J Cancer Res Clin Oncol* 2005;131:205–13.
34. Okabe T, Okamoto I, Tsukioka S, Uchida J, Iwasa T, Yoshida T, Hatashita E, Yamada Y, Satoh T, Tamura K, Fukuoka M, Nakagawa K. Synergistic antitumor effect of S-1 and the epidermal growth factor receptor inhibitor gefitinib in non-small cell lung cancer cell lines: role of gefitinib-induced down-regulation of thymidylate synthase. *Mol Cancer Ther* 2008;7:599–606.
35. Brun Y, Wang XP, Willemot J, Sevenet T, Demenge P. Experimental study of antidiarrheal activity of Salicairine. *Fundam Clin Pharmacol* 1998;12:30–6.
36. Yokoyama Y, Dhanabal M, Griffioen AW, Sukhatme VP, Ramakrishnan S. Synergy between angiostatin and endostatin: inhibition of ovarian cancer growth. *Cancer Res* 2000;60:2190–6.
37. Uchino H, Matsumura Y, Negishi T, Koizumi F, Hayashi T, Honda T, Nishiyama N, Kataoka K, Naito S, Kakizoe T. Cisplatin-incorporating polymeric micelles (NC-6004) can reduce nephrotoxicity and neurotoxicity of cisplatin in rats. *Br J Cancer* 2005;93: 678–87.
38. Okamoto I, Nishimura T, Miyazaki M, Yoshioka H, Kubo A, Takeda K, Ebi N, Sugawara S, Katakami N, Fukuoka M, Nakagawa K. Phase II study of combination therapy with S-1 and irinotecan for advanced non-small cell lung cancer: west Japan thoracic oncology group 3505. *Clin Cancer Res* 2008;14: 5250–4.
39. Inokuchi M, Yamashita T, Yamada H, Kojima K, Ichikawa W, Nihei Z, Kawano T, Sugihara K. Phase I/II study of S-1 combined with irinotecan for metastatic advanced gastric cancer. *Br J Cancer* 2006; 94:1130–5.
40. Takechi T, Okabe H, Ikeda K, Fujioka A, Nakagawa F, Ohshimo H, Kitazato K, Fukushima M. Correlations between antitumor activities of fluoropyrimidines and DPD activity in lung tumor xenografts. *Oncol Rep* 2005;14:33–9.
41. Ohe Y, Sasaki Y, Shinkai T, Eguchi K, Tamura T, Kojima A, Kunikane H, Okamoto H, Karato A, Ohmatsu H, Kanzawa F, Saijo N. Phase I study and pharmacokinetics of CPT-11 with 5-day continuous infusion. *J Natl Cancer Inst* 1992;84:972–4.
42. Masuda N, Fukuoka M, Kusunoki Y, Matsui K, Takifuji N, Kudoh S, Negoro S, Nishioka M, Nakagawa K, Takada M. CPT-11: a new derivative of camptothecin for the treatment of refractory or relapsed small-cell lung cancer. *J Clin Oncol* 1992; 10:1225–9.
43. Ohno R, Okada K, Masaoka T, Kuramoto A, Arima T, Yoshida Y, Ariyoshi H, Ichimaru M, Sakai Y, Oguro M, Ito Y, Morishima Y, et al. An early phase II study of CPT-11: a new derivative of camptothecin, for the treatment of leukemia and lymphoma. *J Clin Oncol* 1990;8:1907–12.
44. Sakuramoto S, Sasako M, Yamaguchi T, Kinoshita T, Fujii M, Nashimoto A, Furukawa H, Nakajima T, Ohashi Y, Imamura H, Higashino M, Yamamura Y, et al. Adjuvant chemotherapy for gastric cancer with S-1, an oral fluoropyrimidine. *N Engl J Med* 2007;357:1810–20.
45. Nagano T, Yasunaga M, Goto K, Koga Y, Kuroda J-i, Nishimura Y, Sugino T, Nishiwaki Y, Matsumura Y. Antitumor activity of NK012 combined with cisplatin against small-cell lung cancer and intestinal mucosal changes in tumor-bearing mouse after treatment. *Clin Cancer Res* 2009;15: 4348–55.

Journal of Controlled Release 142 (2010) 245–250

Contents lists available at ScienceDirect

Journal of Controlled Release

journal homepage: www.elsevier.com/locate/jconrel

Cancer gene therapy by IL-12 gene delivery using liposomal bubbles and tumoral ultrasound exposure

Ryo Suzuki [a,1], Eisuke Namai [a,1], Yusuke Oda [a,1], Norihito Nishiie [a], Shota Otake [a], Risa Koshima [a], Keiichi Hirata [a], Yuichiro Taira [a], Naoki Utoguchi [a], Yoichi Negishi [b], Shinsaku Nakagawa [c], Kazuo Maruyama [a,*]

[a] Department of Biopharmaceutics, School of Pharmaceutical Sciences, Teikyo University, Sagamihara, Kanagawa, Japan
[b] Department of Drug and Gene Delivery System, School of Pharmacy, Tokyo University of Pharmacy and Life Science, Hachioji, Tokyo, Japan
[c] Department of Biotechnology and Therapeutics, Graduate School of Pharmaceutical Sciences, Osaka University, Suita, Osaka, Japan

ARTICLE INFO

Article history:
Received 24 August 2009
Accepted 26 October 2009
Available online 31 October 2009

Keywords:
Interleukin-12 (IL-12)
Ultrasound
Liposomes
Cancer gene therapy
Non-viral vector

ABSTRACT

Interleukin-12 (IL-12) gene therapy is expected to be effective against cancers because it primes the immune system for cancer cells. In this therapy, it is important to induce IL-12 gene expression in the tumor tissue. Sonoporation is an attractive technique for developing non-invasive and non-viral gene delivery systems, but simple sonoporation using only ultrasound is not an effective cancer gene therapy because of the low efficiency of gene delivery. We addressed this problem by combining ultrasound and novel ultrasound-sensitive liposomes (Bubble liposomes) which contain the ultrasound imaging gas perfluoropropane. Our previous work showed that this is an effective gene delivery system, and that Bubble liposome collapse (cavitation) is induced by ultrasound exposure. In this study, we assessed the utility of this system in cancer gene therapy using IL-12 corded plasmid DNA. The combination of Bubble liposomes and ultrasound dramatically suppressed tumor growth. This therapeutic effect was T-cell dependent, requiring mainly $CD8^+$ T lymphocytes in the effector phase, as confirmed by a mouse *in vivo* depletion assay. In addition, migration of $CD8^+$ T cells was observed in the mice, indicating that the combination of Bubble liposomes and ultrasound is a good non-viral vector system in IL-12 cancer gene therapy.

1. Introduction

Interleukin 12 (IL-12), a heterodimeric protein composed of p35 and p40 subunits [1,2], is produced by antigen-presenting cells such as dendritic cells and macrophages. IL-12 has a variety of immunomodulatory anti-tumor effects including induction of interferon-γ (IFN-γ secretion by stimulation of T cells and natural killer (NK) cells, and promotion of cytotoxic T lymphocyte (CTL) maturation [3,4]. In addition, IL-12 induces antiangiogenic effects mainly through IFN-γ-dependent production of the chemokine, interferon-inducible protein-10 (IP-10) [5], suggesting that IL-12 would be an effective anti-tumor agent. Although the systemic administration of IL-12 has been shown to suppress tumor growth, clinical trials were interrupted because of fatal adverse effects [6,7]. On the other hand, local administration of IL-12 into tumors is accepted as a more effective immunotherapeutic approach because of reduced systemic toxicity [8]. In particular, gene therapy by intratumoral injection of the IL-12 gene is expected to be an effective cancer therapy because it would lead to the locally sustained release of IL-12 in the tumor [9].

In cancer gene therapy, it is important to develop easy, safe, efficient and minimally-invasive techniques for transferring genes into tumor tissue. Non-viral gene therapy has many advantages over gene therapy, including ease of plasmid DNA production, lower toxicity and immunogenicity, and lower cost. Many researchers have attempted to develop non-viral gene delivery carriers such as lipids and polymers [10–13]. In addition, there is wide interest in the potential of therapeutic ultrasound for enhancing the efficiency of gene delivery [14,15]. In particular, a physical method using ultrasound combined with nano/microbubbles has many of the desired characteristics for an ideal gene therapy, including low toxicity, the potential for repeated applications, organ specificity, and broad applicability to acoustically accessible organs [16,17]. Ultrasound can create transient nonlethal perforations in cell membranes [18], allowing extracellular plasmid DNA to be directly delivered into the cytosol. The main mechanism of gene delivery is thought to be acoustic cavitation using nano/microbubbles as cavitation nuclei. Based on liposome technology, we previously developed novel liposomal bubbles (Bubble liposomes) containing lipid micelles of the ultrasound imaging gas, perfluoropropane [19–23]. When coupled with ultrasound exposure, Bubble liposomes could

* Corresponding author. 1091-1 Suwarashi, Sagamiko, Sagamihara, Kanagawa 229-0195, Japan. Tel.: +81 42 685 3724; fax: +81 42 685 3432.
E-mail address: maruyama@pharm.teikyo-u.ac.jp (K. Maruyama).
[1] The first three authors contributed equally to this work.

0168-3659/$ – see front matter © 2009 Elsevier B.V. All rights reserved.
doi:10.1016/j.jconrel.2009.10.027

be used as novel gene delivery agents *in vitro* and *in vivo* [19,20,24]. In addition, we found that gene delivery into femoral artery with this method was much more efficient than the conventional lipofection method using Lipofectamine 2000 [19]. And there is little report about cancer gene therapy using nano/microbubbles and ultrasound. Therefore, it is expected that gene delivery using Bubble liposomes and ultrasound will be an effective non-viral vector system for cancer gene therapy. In this study, we assessed this gene delivery system in cancer gene therapy using IL-12 gene.

2. Materials and methods

2.1. Cells and animals

Murine ovarian carcinoma OV-HM cells were kindly provided by Dr. Hiromi Fujiwara. An ovarian tumor OV2944, was induced in a female (C57BL/6 X C3H/He) F_1 mice by giving a single whole-body neutron irradiation, and a cloned line with highly metastatic property (designated OV-HM) was isolated from the parental line [25]. OV-HM cells were grown in RPMI-1640 (Sigma Chemical Co., St. Louis, MO) containing 100 U/ml penicillin (Wako Pure Chemical Industries, Osaka, Japan) and 100 μg/ml streptomycin (Wako Pure Chemical Industries) supplemented with 10% heat-inactivated fetal bovine serum (FBS, GIBCO, Invitrogen Co., Carlsbad, CA). B6C3F1 female mice were obtained from Sankyo Labo Service Corporation, Inc. (Tokyo, Japan) and used at 6 weeks of age. All of the experimental procedures were performed in accordance with the Teikyo University guidelines for the welfare of animals in studies of experimental neoplasia.

2.2. Preparation of Bubble liposomes

Liposomes composed of 1,2-distearoyl-sn-glycero-phosphatidylcholine (DSPC) (NOF Corp., Tokyo, Japan) and 1,2-distearoyl-sn-glycero-3-phosphatidyl-ethanolamine s-methoxypolyethyleneglycol (DSPE-PEG(2 k)-OMe, (PEG, Mw=ca. 2000); NOF) (94:6 (m/m)) were prepared by reverse phase evaporation. Briefly, all reagents (total lipid: 100 μmol) were dissolved in 8 ml of 1:1 (v/v) chloroform/diisopropyl ether, and then 4 ml of phosphate buffered saline (PBS) was added. The mixture was sonicated and evaporated at 65 °C. The organic solvent was completely removed, and the size of the liposomes was adjusted to less than 200 nm using an extruding apparatus (Northern Lipids Inc., Vancouver, Canada) and sizing filters (pore sizes: 100 and 200 nm; Nuclepore Track-Etch Membrane, Whatman plc, UK). After sizing, the liposomes were sterilized by passing them through a 0.45-μm pore size filter (Millex HV filter unit, Durapore PVDF membrane, Millipore Corp., MA). The size of the liposomes was measured by dynamic light scattering (ELS-800, Otsuka Electronics Co., Ltd., Osaka, Japan). The average diameter of these liposomes was between 150 and 200 nm. Lipid concentration was measured using the Phospholipid C test (Wako Pure Chemical Industries). Bubble liposomes were prepared from the liposomes and perfluoropropane gas (Takachiho Chemical Industrial Co., Ltd., Tokyo, Japan). Briefly, 5-ml sterilized vials containing 2 ml of the liposome suspension (lipid concentration: 2 mg/ml) were filled with perfluoropropane, capped, and then supercharged with 7.5 ml of perfluoropropane. The vial was placed in a bath-type sonicator (42 kHz, 100 W; Bransonic 2510 J-DTH, Branson Ultrasonics Co., Danbury, CT) for 5 min to form the Bubble liposomes. In this method, the liposomes were reconstituted by sonication and supercharged with perfluoropropane in the 5-mL vial container. Perfluoropropane was entrapped within the lipid micelles, comprising DSPC and DSPE-PEG (2 k)-OMe, to form nanobubbles. The lipid nanobubbles were encapsulated within the reconstituted liposomes, which now ranged in size from around 500 nm–1 μm, compared to 150–200 nm before supercharging with perfluoproropane.

2.3. Plasmid DNA vector construction

The plasmid pCMV-Luc contained the firefly luciferase gene of pGL3-control (Promega) at the *HindIII/XbaI* site of the pcDNA3 vector (Invitrogen). This plasmid was an expression vector encoding the firefly luciferase gene under the control of a cytomegalovirus promoter. The plasmid pCMV-IL12 contained murine IL-12, derived from mIL-12 BIA/pBluescript II KS(−) (kindly provided by Dr. Yamamoto, Department of Immunology, Graduate School of Pharmaceutical Sciences, Osaka University, Japan) in the *XhoI/NotI* site of the pHMCMV5 vector. This expression vector encoded the murine IL-12 gene under the control of a cytomegalovirus promoter [26].

2.4. Intratumoral administration of plasmid DNA

B6C3F1 mice were intradermally inoculated with OV-HM cells (1×10^6 cells/mouse) in the flank. After 7 days, a suspension (25 μL/mouse) of Bubble liposomes (2.5 μg) and pCMV-Luc or pCMV-IL12 (10 μg) was injected into the tumor, and ultrasound (1 MHz, 0.7 W/cm^2, 60 s) was transdermally applied to the tumor tissue. A conventional lipofection method was also investigated. A suspension (25 μL/mouse) of Lipofectamine 2000 (20 μg) and pCMV-Luc or pCMV-IL12 (10 μg) were incubated together for 20 min to allow them to complex. Then the complex was injected into the tumor. All treatment groups consisted of five mice.

2.5. Luciferase assay

Each day after the pCMV-Luc injection, mice were sacrificed and the tumor tissue was recovered. The tumor tissue was homogenized in lysis buffer (0.1% Triton X-100, 0.1 M Tris–HCl pH 7.8, 2 mM EDTA) and frozen (−80 °C) and thawed at room temperature twice. The homogenized tumor tissue was centrifuged (12,000 rpm, 4 °C, 10 min) and the supernatant was recovered for the luciferase assay. Luciferase activity was measured using a luciferase assay system (Promega) and luminometer (TD-20/20, Turner Designs, Sunnyvale, CA). The activity was measured as relative light units (RLU) per milligram protein.

2.6. Reverse transcription-polymerase chain reaction (RT-PCR) analysis for IL-12 expression in tumor tissues

OV-HM tumors were collected 1 or 2 days after intratumoral injection of pCMV-IL12 and Bubble liposomes, and total RNA was isolated using ISOGEN according to the manufacturer's instructions and dissolved with 20 μL TE buffer. RT proceeded for 60 min at 42 °C in 20 μl reaction mixture containing 1 μg total RNA treated with DNase I, 5 mM $MgCl_2$, RNA PCR buffer (Takara Bio, Kyoto, Japan), 1 mM dNTP mix, 0.125 μM Oligo dT-Adaptor primer (Takara Bio), 0.5 U/μL RNase inhibitor and 0.25 U/μL AMV reverse transcriptase XL (Takara Bio). PCR amplification of IL-12 and β-actin transcripts was performed in 20 μL reaction mixture containing 2 μL RT-material, PCR buffer, 0.5 U Takara Ex Taq HS, 0.2 mM dNTP, 2.5 mM $MgCl_2$, and 0.4 mM primers. The sequences of the specific primers were as follows: murine IL-12: forward, 5′-ctc acc tgt gac acg cct ga-3′; reverse, 5′-cag gac act gaa tac ttc tc-3′; and murine β-actin: forward, 5′-tgt gat ggt ggg aat ggg tca g-3′; reverse, 5′-ttt gat gtc acg cac gat ttc c-3′. After denaturation for 5 min at 95 °C, three sequential steps, denaturation for 45 s at 95 °C, annealing for 60 s at 48 °C, and extension for 2 min at 72 °C, were repeated for 40 cycles, with a final extension step for 4 min at 72 °C.

EZ Load (Bio-Rad Laboratories, Inc., Tokyo, Japan) was used as a 100-bp molecular ladder. The PCR products were electrophoresed through a 2% agarose gel, stained with ethidium bromide, and visualized under ultraviolet radiation. The expected PCR product sizes were 430 bp (IL-12) and 514 bp (β-actin).

2.7. Anti-tumor effect of intratumoral administration on IL-12 gene expression in mice

B6C3F1 mice were intradermally inoculated with OV-HM cells (1×10^6 cells/mouse) into the flank. For single therapy, established tumors with diameters of 8–10 mm were injected with a suspension (25 μL/mouse) of Bubble liposomes (2.5 μg) and pCMV-IL12 (10 μg), and ultrasound (1 MHz, 0.7 W/cm^2, 60 s) was transdermally applied to the tumor tissue. We also examined the intratumoral injection of a complex (25 μL/mouse) of Lipofectamine 2000 (20 μg) and pCMV-IL12 (10 μg) as a conventional lipofection method for comparison. For repetitive therapy, the mice were treated as above on days 0, 2, 5, 7, 9 and 12 after first treatment. The anti-tumor effects were evaluated by measuring tumor volume. Tumor volume was calculated using the formula: (major axis × minor axis^2) × 0.5. All data are expressed as relative tumor volume to that before the first treatment. All treated groups contained five mice.

2.8. In vivo depletion analysis

GK1.5 hybridoma (rat anti-mouse CD4 mAb) and 53-6.72 hybridoma (rat anti-mouse CD8 mAb) were purchased from American Type Culture Collection (ATCC) (Manassas, VA). Ascites from BALB/c nude mice intraperitoneally injected with each hybridoma were collected, and antibodies were purified using a protein A column (GE Healthcare, Pollards Wood, UK). Mice bearing OV-HM were intratumorally injected with pCMV-IL12 and Bubble liposomes on days 0, 2, 5, 7, 9 and 12 after the first treatment. Additionally, the mice were intraperitoneally injected four times on days −3, 4, 11 and 18 after the first treatment with 100 μg/mouse of anti-mouse CD8 mAb for CD8$^+$ cells or anti-mouse CD4 antibody for CD4$^+$ cells, or on days −3, −2, −1, 0, 5, 10, 15 and 20 after the first treatment with 200 μg/mouse of anti asialoGM1 mAb (Wako Pure Chemical Industries) for NK cells. The depletion of T-cell subsets and NK cells was confirmed by flow cytometric analysis of peripheral blood. Tumor growth was monitored as described above.

2.9. Immunohistochemical analysis

B6C3F1 mice were intradermally inoculated with OV-HM cells (1×10^6 cells/mouse) into the flank. After 7, 9 or12 days, a suspension (25 μL/mouse) of Bubble liposomes (2.5 μg) and pCMV-IL12 (10 μg) was injected into the tumor, and ultrasound (1 MHz, 0.7 W/cm^2, 60 s) was transdermally applied to the tumor tissue. After 13 days of tumor inoculation, the mice were sacrificed, and the tumor tissue was dissected and then embedded in the OCT compound. Frozen sections (10 μm thick) were fixed with 4% paraformaldehyde at 4 °C for 10 min, and treated with 0.3% H_2O_2 in methanol:PBS (1:1) for 15 min and 1.5% normal cow serum in PBS for 10 min at room temperature. The sections were treated with rat anti-mouse CD8 mAbs (1:100) or rat anti-mouse perforin mAbs (1:100) (Kamiya Biomedical Co., Seattle, WA) in PBS containing 0.1% BSA at 4 °C overnight. The section was washed and treated with horse radish peroxidase-conjugated goat anti-rat IgG Abs (1:500) in PBS containing 0.1% BSA at room temperature for. 2 h. The diaminobenzidine-reaction system (Vector Laboratories, Burlingame, CA) was used to stain the sections. We also stained the sections with hematoxylin solution for counterstaining. The samples were observed with a microscope (IX-71, Olympus, Tokyo, Japan).

2.10. Statistical analysis

Differences between experimental groups were compared with non-repeated measures ANOVA and Dunnett's test.

3. Results

3.1. Bubble liposomes and ultrasound-mediated gene delivery into solid tumors

To evaluate the effectiveness of gene delivery with Bubble liposomes and ultrasound into OV-HM solid tumors, we utilized the luciferase reporter gene expression assay (Fig. 1a). The effectiveness of gene delivery with conventional lipofection using Lipofectamine 2000 was also examined. Luciferase expression with ultrasound or Bubble liposomes was low, and even lower with Lipofectamine 2000. On the other hand, luciferase expression with the combination of Bubble liposomes and ultrasound exposure was higher than in the other groups. Therefore, the profile of luciferase expression was measured in mice treated with Bubble liposomes and ultrasound. Luciferase expression gradually decreased after transfection (Fig. 1b), with the elimination rate constant (Ke) and half period ($T_{1/2}$) of gene expression being 1.26 days^{-1} and 0.54 days, respectively.

3.2. IL-12 gene expression in solid tumors transfected with IL-12 corded plasmid DNA using Bubble liposomes and ultrasound

To assess IL-12 expression in solid tumors transfected with IL-12 corded plasmid DNA (pCMV-IL12), the expression of IL-12p40 mRNA was examined with RT-PCR (Fig. 2). No expression of IL-12p40 mRNA in solid tumors transfected with pCMV-IL12 was observed. A small amount of IL-12p40 mRNA was expressed in solid tumors transfected with pCMV-IL12 using Lipofectamine 2000 on 1 day after gene transfection. On the other hand, the expression of IL-12p40 mRNA was observed in solid tumors transfected with pCMV-IL12 using Bubble liposomes and ultrasound for at least 2 days after gene transfection. This result indicates that IL-12 is expressed more effectively in solid tumors transfected using Bubble liposomes and ultrasound than using Lipofectamine 2000.

3.3. Anti-tumor effect of IL-12 gene delivery with Bubble liposomes and ultrasound

First, we examined the effect of a single delivery of IL-12 gene (Fig. 3a). Gene delivery using Bubble liposomes, ultrasound or

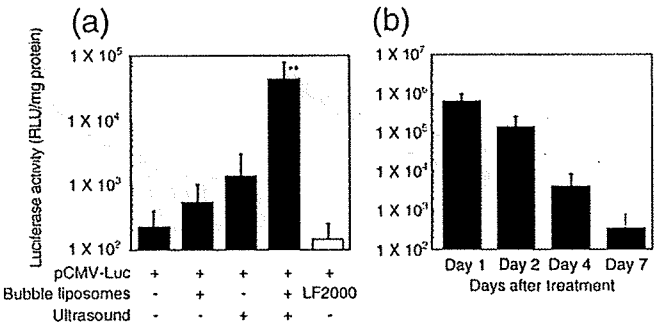

Fig. 1. Gene expression profiles in solid tumors following gene delivery with Bubble liposomes and ultrasound. Comparison of gene expression efficiency by gene delivery with each gene delivery method. B6C3F1 mice were intradermally inoculated with 1×10^6 OV-HM cells into the flank. Seven days after inoculation, the tumors were injected with pCMV-Luc (10 μg) using Bubble liposomes (2.5 μg) and/or ultrasound (1 MHz, 0.7 W/cm^2, 1 min), or Lipofectamine 2000 as a conventional lipofection method. (a) Two days after gene delivery, the mice were sacrificed and luciferase expression was measured in the solid tumor tissue. The data represent means ± SD ($n=3$). (b) Time course of luciferase expression after gene delivery with Bubble liposomes and ultrasound. Luciferase expression was measured at each time point after pCMV-Luc delivery into the solid tumor with Bubble liposomes and ultrasound exposure. **$P<0.01$ compared to the group treated with plasmid DNA, Bubble liposomes, ultrasound or LF2000. LF2000: Lipofectamine 2000.

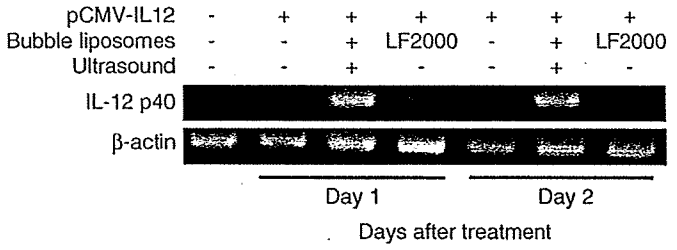

Fig. 2. RT-PCR analysis of IL-12 expression in solid tumors after pCMV-IL12 gene delivery. B6C3F1 mice were intradermally inoculated with 1×10^6 OV-HM cells into the flank. Seven days after inoculation, the tumors were injected with pCMV-IL12 (10 μg) using Bubble liposomes (2.5 μg) and/or ultrasound (1 MHz, 0.7 W/cm^2, 1 min), or Lipofectamine 2000 as a conventional lipofection method. One or 2 days after gene delivery, the mice were sacrificed, total RNA was prepared from the tumors, then RT-PCR was performed using a specific IL-12 primer as described in Materials and Methods. The PCR products were electrophoresed though a 3% agarose gel and stained with EtBr. To ensure the quality of the procedure, RT-PCR was performed on the same sample using a specific β-actin primer. LF2000: Lipofectamine 2000.

Lipofectamine 2000 showed no apparent anti-tumor effect, as was found for pCMV-Luc intratumoral delivery using Bubble liposomes and ultrasound. In contrast, the growth of OV-HM tumors was dramatically suppressed in mice treated by pCMV-IL12 intratumoral delivery using Bubble liposomes and ultrasound; however, complete regression was not observed. Thus, we examined the effect of repetitive IL-12 gene therapy to obtain more effective therapeutic effects (Fig. 3b). Gene delivery using Bubble liposomes, ultrasound or Lipofectamine 2000 showed no apparent anti-tumor effect, even in repetitive therapy. In contrast, IL-12 gene delivery using the combination of Bubble liposomes and ultrasound effectively suppressed tumors, and complete regression occurred in 80% of the tumor-bearing mice. There was no decrease in body weight of these mice as a side effect of IL-12 cancer therapy (data not shown). In addition, this group of mice demonstrated prolonged survival, indicating that OV-HM cells were effectively killed by IL-12 gene therapy with Bubble liposomes and ultrasound.

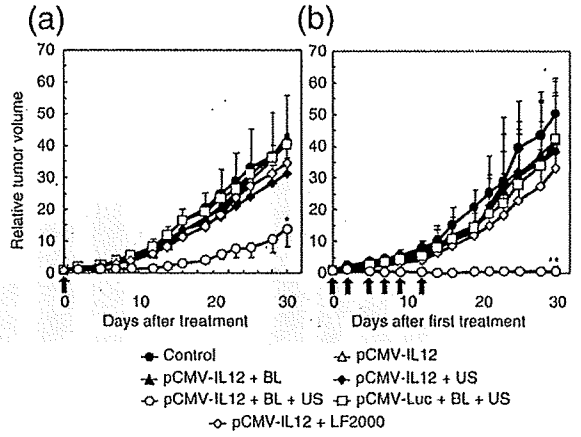

Fig. 3. Anti-tumor effect of IL-12 gene delivery. B6C3F1 mice were intradermally inoculated with 1×10^6 OV-HM cells into the flank. (a) Single gene therapy. (b) Repetitive gene therapy. Each day (arrows) after first treatment, the tumors were injected with pCMV-IL12 (10 μg) using Bubble liposomes (2.5 μg) and/or ultrasound (1 MHz, 0.7 W/cm^2, 1 min), or Lipofectamine 2000 as a conventional lipofection method. The volume of the growing tumors was calculated by: (tumor volume; mm^3) = (major axis; mm) × (minor axis; mm)^2 × 0.5). The data are represented as tumor volume relative to the tumor volume on the first day of treatment (day 7 after tumor inoculation). Arrow shows days of treatment. Each point represents the mean ± SD ($n = 5$). *$P < 0.05$ or **$P < 0.01$ compared to the group treated with pCMV-IL12, pCMV-IL12 + BL, US or LF2000 or pCMV-Luc + BL + US. BL: Bubble liposomes, US: Ultrasound, LF2000: Lipofectamine 2000.

3.4. Determination of immune subsets responsible for tumor regression induced by IL-12 gene delivery using Bubble liposomes and ultrasound

To investigate the anti-tumor mechanism of intratumoral pCMV-IL12 delivery using Bubble liposomes and ultrasound, we examined the individual contribution of CD4$^+$ and CD8$^+$ T cells and NK cells (Fig. 4). The anti-tumor effects of pCMV-IL12 delivery using Bubble liposomes and ultrasound were attenuated by the depletion of CD8$^+$ T cells and CD4$^+$ T cells. The depletion of CD8$^+$ T cells effectively blocked the anti-tumor effect. Also, the anti-tumor effect was blocked in mice that were depleted of both CD4$^+$ and CD8$^+$ T cells. On the other hand, the tumor growth suppressing effects were not affected by NK cell depletion. Therefore, we concluded that CD8$^+$ CTLs, activated by the helper function of CD4$^+$ T cells, were the predominant effector cells in this therapeutic system. CD4$^+$ cells alone also partly contributed to the enhanced anti-tumor effect.

To investigate the infiltration of CD8$^+$ T cells into tumor tissues containing the IL-12 gene delivered using Bubble liposomes and ultrasound, tumor tissues were subjected to immunohistochemical staining for CD8 (Fig. 5a–c). Tumor tissue from untreated mice, or mice treated with the IL-12 gene delivered using Bubble liposomes and ultrasound, showed increased accumulation of CD8$^+$ T cells compared to control mice treated with the luciferase gene, delivered using Bubble liposomes and ultrasound. In addition, we examined the activation states of tumor-infiltrating T cells by immunohistochemical analysis for perforin, the major cytotoxic molecule in activated CTLs (Fig. 5d–f). Tumor tissue to which the IL-12 gene had been delivered using Bubble liposomes and ultrasound exhibited significantly higher numbers of perforin-positive cells than non-treated tumor tissue, or tissue treated with luciferase gene.

4. Discussion

There are two main therapeutic strategies in cancer gene therapy. One approach is to cause a direct effect on cancer cells by delivering suicide genes such as herpes simplex virus thymidine kinase, [27] siRNA for oncogenes, [28] and proteins associated with the cell cycle [29] and apoptosis [30,31]. In this approach, it is necessary to deliver the therapeutic gene into most of the cancer cells to induce cytotoxicity. The second approach is indirect and activates anti-tumor immunity mediated by the delivery of a cytokine gene such as IL-12. In such cytokine gene therapy, the therapeutic gene does not have to be delivered into all the cancer cells since the cytokine is secreted from the cells. Therefore, a local supply of IL-12 in tumors is

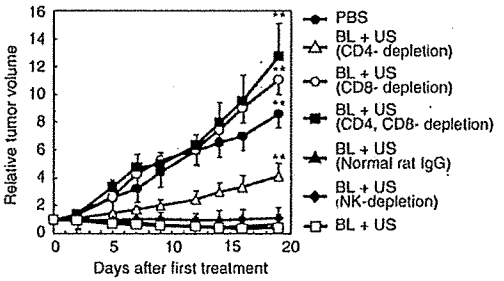

Fig. 4. Determination of immune subsets responsible for the anti-tumor effect induced by IL-12 gene delivery with Bubble liposomes and ultrasound. B6C3F1 mice were intradermally inoculated with 1×10^6 OV-HM cells into the flank. For depletion of CD4$^+$ T cells, CD8$^+$ T cells or NK cells in the mice, GK1.5 ascites (anti-CD4), 53-6.72 ascites (anti-CD8) or anti-asialoGM1 antisera was intraperitoneally injected as described in Materials and methods. On 0, 2, 5, 7, 9 or 12 days after first treatment, IL-12 gene therapy was performed with Bubble liposomes and ultrasound. The data represent the tumor volume relative to the tumor volume on the first day of treatment (day 7 after tumor inoculation). Each point represents the mean ± SD ($n = 5$). **$P < 0.01$ compared to the group treated with BL + US (Non-depletion). BL: Bubble liposomes, US: Ultrasound.

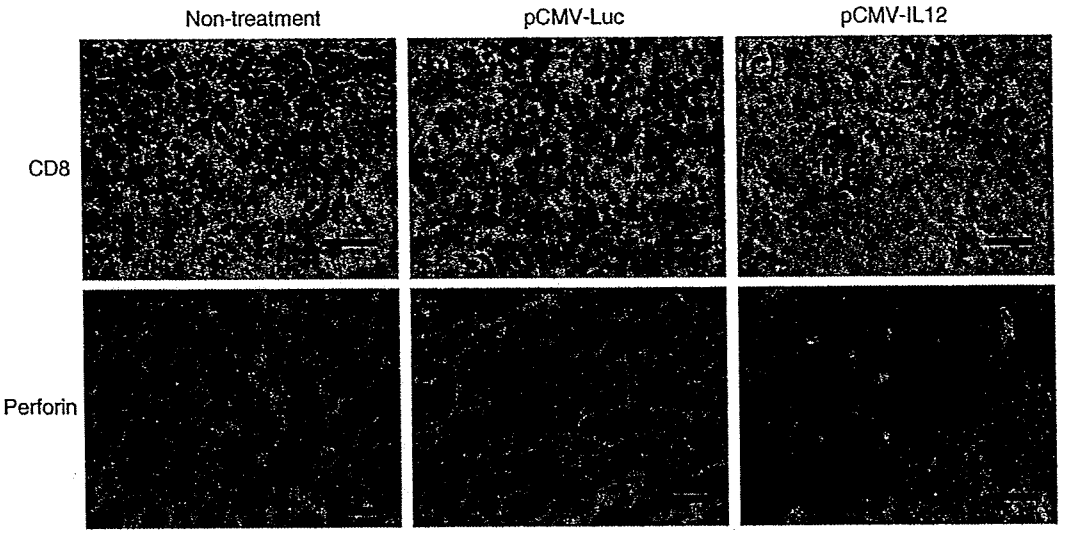

Fig. 5. Images of infiltrating T cells in OV-HM tumors following pCMV-IL12 delivery using Bubble liposomes and ultrasound. B6C3F1 mice were intradermally inoculated with 1×10^6 OV-HM cells into the flank. Seven, 9 or12 days after tumor inoculation, the tumors were injected with pCMV-Luc (b and e) or pCMV-IL12 (c and f) using Bubble liposomes and ultrasound. On day 13 after tumor inoculation, immunohistochemical staining against CD8 (a, b and c) and perforin (d, e and f) was performed using frozen tumor sections. Scale bar shows 10 μm.

an effective immunotherapeutic approach with reduced systemic adverse effects. Many anti-tumor effects depend on this method for IL-12 gene delivery. Viral vector systems have high potency and are effective for gene delivery, but gene therapy using viral vector systems may have associated safety issues [32]. Although transfection efficiency of most non-viral vector systems is lower, they are generally considered safer than viral vector systems [33]. Therefore, non-viral vector systems are preferred to cancer gene therapy using cytokines because it is not necessary to deliver the cytokine gene into all the cells. There have been many recent reports about gene delivery using the combination of nano/microbubbles and ultrasound [16–18], but most of them only confirmed the efficiency of gene expression using reporter genes. On the other hand, there have been few reports regarding therapeutic effects using sonoporation technology in cancer gene therapy. In this study, we assessed the effectiveness of the combination of Bubble liposomes and ultrasound as a non-viral vector system for effective cancer gene therapy, using plasmid DNA expressing IL-12, a potent primer of anti-tumor immunity.

IL-12 expression by IL-12 corded plasmid DNA delivery with the combination of Bubble liposomes and ultrasound was higher than that with a conventional lipofection method using Lipofectamine 2000 (Fig. 2). The therapeutic effect of IL-12 cancer gene therapy using each gene delivery method was compared (Fig. 3). IL-12 gene delivery with Lipofectamine 2000 did not suppress tumor growth, whereas gene delivery using a combination of Bubble liposomes and ultrasound effectively suppressed tumor growth. We originally thought that this was due to the level of IL-12 expression (Fig. 2), but complete tumor rejection was not observed in any mice treated with IL-12 gene delivery using Bubble liposomes and ultrasound (Fig. 3a), perhaps because the IL-12 gene is only transiently expressed in the tumor tissue. To address this problem, the IL-12 gene was repeatedly delivered using Bubble liposomes and ultrasound: as shown in Fig. 3b, the tumors were completely rejected. This complete rejection was attributed to the maintenance of therapeutic IL-12 levels in the tumor tissue. On the other hand, we could not observe anti-tumor effect in the luciferase corded plasmid DNA (pCMV-Luc) delivery with Bubble liposomes and ultrasound. This result not only suggests that IL-12 expression was important to suppress tumor growth but also suggests that there was no effect on tumor suppression by the combination of Bubble liposomes and ultrasound. In addition, we used Lipofectamine 2000 as control because gene transfection with intraperitoneal injection of Lipofectamine 2000 could effectively deliver into ascites tumor cells in our previous report [20]. Therefore, in this case of local tumoral injection, we thought that Lipofectamine 2000 could also be utilized as control vector system. Moreover, our collaborator reported about anti-tumor effects by single intratumoral injection of IL-12 expressing RGD fiber mutant adenovirus vector in OV-HM tumor bearing mice. In the report, tumor growth was suppressed and the tumor regression rate was about 40% [9]. In our study, although effective tumor growth suppression was observed in the therapeutic mice by single injection of IL-12 gene with Bubble liposomes and ultrasound, the tumor regressing mice were not observed. In this single therapy, our system was not equal to adenovirus vector in terms of tumor regression rate. On the other hand, the tumor regression rate in our repetitive therapy reached to 80%. And anti-tumor effect by repetitive therapy in our gene delivery system could go beyond that by single therapy with adenovirus vector. From these results, it was thought that the combination of Bubble liposomes and ultrasound might be a useful non-viral vector system for cancer gene therapy.

The anti-tumor effect by gene delivery with the combination of Bubble liposomes and ultrasound completely disappeared in mice lacking $CD8^+$ T lymphocytes (Fig. 4). Therefore, in this IL-12 gene therapy, $CD8^+$ T lymphocytes play a major role in suppressing tumor growth, suggesting that the combination of Bubble liposomes and ultrasound can effectively induce sufficient IL-12 expression to cause anti-tumor immune responses. In the Fig. 4, $CD8^+$ T lymphocytes depletion and $CD4^+$ and $CD8^+$ T lymphocytes depletion rather enhanced tumor growth. We thought that this reason was a same phenomenon as increasing the frequency of tumor generation according to decrease anti-tumor activity of immune competent cells by immunosuppressive agents. In brief, the balance of tumor growth and tumor rejection by immune system trend toward tumor growth by the depletion of $CD4^+$ and $CD8^+$ T lymphocytes. Therefore, it was thought that tumor growth was accelerated by the depletion. In other report, same phenomenon was observed [34]. The invasion of many $CD8^+$ T lymphocytes was observed in tumor tissue from mice treated with the IL-12 gene, Bubble liposomes and ultrasound (Fig. 5c), and perforin-positive cells were also observed in this tumor tissue (Fig. 5f). These results suggest that the expression of IL-12 genes, delivered using Bubble liposomes and ultrasound, primed the anti-tumor immunity, causing the tumor cells to be rejected. In this study, we did not measure the IL-12 concentration in the tumor tissue, but Colombo et al. reported that 30–80 pg/ml IL-12 at the tumor site can induce 40% regression of